ISSN 0280-5316
ISRN LUTFD2/TFRT--5856--SE

Road Slope Estimation using a Longitudinal Accelerometer and Kalman Filtering

Tobias Bonnedahl

Department of Automatic Control
Lund University
April 2010

Lund University
Department of Automatic Control
Box 118
SE-221 00 Lund Sweden

Document name
MASTER THESIS

Date of issue
April 2010

Document Number
ISRN LUTFD2/TFRT--5856--SE

Author(s)
Tobias Bonnedahl

Supervisor
Fredrik Nilsson and Håkan Jonsson Scania AB, Södertälje
Karl-Erik Årzén Automatic Control, Lund (Examiner)

Sponsoring organization

Title and subtitle
Road Slope Estimation using a Longitudinal Accelerometer and Kalman Filtering (Estimering av vägbanelutning med accelerometer och Kalmanfilter)

Abstract
Heavy-duty vehicles of today consist of much electronics and many sensors. One of these sensors is a longitudinal accelerometer. This Master's thesis investigates the possibilities to determine the road slope angle with a longitudinal accelerometer. With the knowledge of current road slope angle, many other control systems in the trucks can be improved. The optimization of these control systems are important in order to maximize safety and minimize fuel consumption. The work consisted of developing an observer for estimating the road slope angle and tuning it until the results were satisfying. The estimations are made with a Kalman filter. Improvements obtained with fixed lag smoothing are also investigated. The results obtained in the thesis show that the road slope angle can be estimated with a longitudinal accelerometer. The results are satisfying, except during powerful retardations. A solution for improvement in these scenarios is presented. The solution consists of changing the dynamics of the estimations when a retardation is detected.

Keywords

Classification system and/or index terms (if any)

Supplementary bibliographical information

ISSN and key title
0280-5316

ISBN

Language
English

Number of pages
66

Recipient's notes

Security classification

Acknowledgements

I would like to thank everyone at the departments REVB, REVC and RTCS at Scania for making me feel welcome during my work done in November 2009 to April 2010. You have all contributed in making it an enjoyable and memorable stay.

I am most grateful of my supervisors Fredrik Nilsson and Håkan Jonsson at Scania for the support you have given me during this thesis. I also appreciate the support given by Jolle Ijkema on the questions regarding vehicle dynamics, and for the time you have taken to help me.

Furthermore, I would like to thank all my friends in Lund for the unforgettable years, and my family for the support given to me during my education.

Contents

1 Introduction

In this chapter, the background and objectives of the thesis are laid out. The limitations of the thesis are also presented.

1.1 Background

Many systems in a heavy-duty vehicle of today contain a longitudinal accelerometer. This specific accelerometer has not had a real area of application. A brief investigation was made by [13] to investigate what the signal from it could be used for. The resulting report showed that the signal could be used to estimate the road slope angle.

By knowing the road slope angle, the largest benefit for trucks used for long-haul is the optimization of cruise-control and fuel-efficiency. For construction vehicles, that are used in areas where the standards that are mentioned in Section 2.4 do not apply, the largest benefit lies in finding an appropriate starting gear.

1.1.1 Benefits of an accurate road slope estimation

An accurate road slope estimation could mean that the vehicle will be safer and more fuel efficient. This is very important, especially to trucks. Trucks are used to freight many tonnes and therefore, has a larger fuel consumption than a passenger car, which means that more can be done to improve it. By knowing the present road slope angle, a cruise control will be able to be more accurate and to minimize fuel consumption.

Improved traction and brake control are also important aspects. With the knowledge of the road's incline during a powerful retardation, the brake power can be distributed to where it is needed. Furthermore, a fully loaded vehicle with the wrong choice of start gear in a slope can have terrible consequences. By knowing the current road slope angle, as well as the weight of the carriage, an appropriate gear can be chosen.

1.2 Objectives

The aim of this thesis is to create a model for estimation of road slope angle in Matlab/Simulink by using a longitudinal accelerometer. The idea is to eventually implement it in real-time in the truck. The estimations are made with different versions of the Kalman filter.

1.3 Limitations

This section presents the limitations and properties not taken into consideration in the road slope model.

1.3.1 Trailers

How the estimation is affected when a tractor is used in combination with a trailer is not investigated in this thesis.

1.3.2 Steep downhill slopes

How the estimation behaves in steep downhill slopes will not be investigated. The reason is that there were no appropriate slopes available. The steepest downhill slope tested in this thesis is 8 %.

1.4 Outline of the report

In Chapter 2, the theory behind the Kalman filter is presented in the first section. The following section covers vehicle dynamics. The chapter is then concluded with a section concerning road building.

The method is elaborated in Chapter 3, first with a section about the data collecting. Then, with a section regarding the model used for the estimation. The last section of the chapter explains the Kalman filter design.

The results from the estimations, and comparisons with GPS-data, are presented in Chapter 4. The chapter is divided into five sections, each one concerning a different driving scenario.

Conclusions drawn from the results are laid out in Chapter 5. The chapter starts with a few general conclusion on the model, followed by specific conclusions in the various driving scenarios.

In Chapter 6, the problems that occurred during the thesis are elaborated. To some of the problems, solutions are presented.

The work left to be done is laid out in Chapter 7. Suggestions of ways to extend the model are presented.

2 Theory

In this thesis, the estimations are done with a Kalman filter. The theory behind the Kalman filter is described in this chapter. After that, vehicle dynamics in general, as well as some individual properties of the trucks used for collecting the data, are described in the following sections. The main theory behind how a road is built, with focus on inclines, concludes this chapter.

2.1 Kalman filter

The Kalman filter was developed by Rudolf E. Kalman in 1960 [2]. The algorithm is an important tool in signal processing, mainly due to the large sector of application. The filter is used in many applications involving navigation in marine, land and aerospace, where e.g. the velocity and position of an aircraft can be estimated [1].

It is also very attractive in control theory, where an accurate estimate of certain states has to be made in order to develop a controller. The filter is designed to minimize the mean square error and therefore, it is considered to be optimal for linear systems with Gaussian noise [2].

Another advantage with the Kalman filter is that the model is written in state space form, which is convenient since the signals are allowed to be vectors. Having the model in state space form will also allow the filter to handle time invariant systems, transients and finite measures. The possibility to weigh signals to each other is another important feature of the Kalman filter [4].

The Kalman filter is mainly used to estimate the past, present or future states in a process. The Kalman filter can be adjusted to handle both discrete and continuous signals, as well as linear and non-linear systems. When the filter is changed to handle non-linear systems, it is called *Extended Kalman filter* [3].

As mentioned earlier, the Kalman filter is used to estimate the states of a system. In Eq. 2.1 and Eq. 2.2, a discrete system is shown on state space form.

$$x_{k+1} = Ax_k + Bu_k + w_{1_k} \tag{2.1}$$

$$z_k = Cx_k + Du_k + w_{2_k}, \tag{2.2}$$

where k corresponds to the time index, x_k is the state vector, u_k is the control signal and z_k is the measured signals. A, B, C and D are the matrices that describe the system, or the process, of which the filter is to be applied on.

The matrix A decides how the previous states, x_k, are being translated into the new states, x_{k+1}. The matrix B determines how the control signal will be included in the system, and C decides how the states effect the measured signals. The matrix D corresponds to a direct term between the control signal and the measured signals, and is often set to zero. All three of the remaining matrices, A, B and C, can vary with time, but are, in most applications assumed to be constant [2].

The vectors w_{1_k} and w_{2_k} are uncorrelated, zero mean, Gaussian distributed random variables and correspond to process and measurement noise respectively

$$w_{1_k} \in N(0, Q_k) \tag{2.3}$$
$$w_{2_k} \in N(0, R_k). \tag{2.4}$$

The matrices Q_k and R_k are the process noise covariance and measurement noise covariance respectively, as seen in Eq. 2.5 and Eq. 2.6. These are the main design parameters of the filter [1].

$$Q_k = E(w_{1_k} w_{1_k}^T) \tag{2.5}$$
$$R_k = E(w_{2_k} w_{2_k}^T) \tag{2.6}$$

The matrices Q_k and R_k are often constant, and simply denoted Q and R.

The choice of Q and R is a compromise between the Kalman filter's response time and sensitivity to noise. A large Q corresponds to much process noise, where it is important to weigh in the measurements y_k. This means that the measurement noise w_{2_k} is also amplified, which is not wanted. But the filter obtained is very fast to react to changes in the signals, which is sometimes needed. One can say that the matrix Q determines how much the state are allowed to change from one sample to the next. On the other hand, if the matrix R is large, the noise is not amplified, but the filter will respond slowly to changes. The compromise between a fast, noise sensitive filter and a noise robust filter, which is slow to converge, has to be made with the individual system in mind [1].

The state vector x_k is estimated from the measured signals y_k, even though the signals are corrupted with the measurement noise w_{2_k}. The estimate is denoted $\hat{x}_{k|\tau}$. This notation corresponds to an estimate of the state vector x at time k based on the available information at time up to time τ. Different values of τ relative k give the filter different properties [1].

- $k = \tau$: Filtering
- $k > \tau$: Prediction

- $k < \tau$: Fixed lag smoothing

Both prediction and fixed lag smoothing are of great importance for many applications, and the latter will be explained in Section 2.1.2.

To minimize the mean square error, i.e. the squared difference between the true state and the estimate, $\tilde{x}_k = x_k - \hat{x}_k$, is fed back through the system [1].

This yields

$$\hat{x}_{k+1} = A\hat{x}_k + Bu_k + K(y_k - \hat{y}_k) \tag{2.7}$$
$$\hat{y}_k = C\hat{x}_k. \tag{2.8}$$

When the Kalman filter is running, two alternating steps are run. The initiation of the filter starts at the time update, which is followed by the correction, where the measurement update is made. After the measurement update is made, the time update runs again [1].

The time update,

$$\hat{x}_{k+1|k} = A\hat{x}_{k|k} + Bu_k \tag{2.9}$$
$$P_{k+1|k} = AP_{k|k}A^T + Q, \tag{2.10}$$

starts by predicting the states one sample a head, called *a priori estimate*, based on the previous estimate of the state and the current value of the input. After that, the estimation error covariance matrix $P_{k+1|k}$ is calculated [1].

The measurement update,

$$K_{k|k} = P_{k|k-1}C^T[CP_{k|k-1}C^T + R]^{-1} \tag{2.11}$$
$$\hat{x}_{k|k} = \hat{x}_{k|k-1} + K_k(y_k - C\hat{x}_{k|k-1})) \tag{2.12}$$
$$P_{k|k} = P_{k|k-1} - K_kCP_{k|k-1}, \tag{2.13}$$

starts with computing the new Kalman gain K_k with the calculated P_k from the time update. After that, the states are updated with the new measurement y_k and the newly calculated gain, and last the error covariance matrix P_k is updated with the new value of the gain K_k [1].

By looking at these equations, a few properties can be noticed. Inspection of Eq. 2.11 shows that if the system has a lot of measurement noise, i.e. R is large, the gain K_k will be small. This means that the measurement y_k will not be given much credibility when the next estimation is being calculated. On the other hand, if the measurement noise is small, the filter will have a large gain and the measurements will be given a lot of credibility [4].

2.1.1 Steady-state

The filter parameters K_k and P_k will very soon after the filter is initiated and any contingent transients are removed by the system, converge to a constant value. This is called *steady-state*, and the matrices are denoted K_p and P_p. For real-time applications, this is very important since these values can be calculated in advance and by doing so, minimize the computational effort needed when the filter is running. It is said that the parameters are calculated *offline*.

By simulating the system, the values of K_p and P_p can be found after they have converged to the steady-state values. This is equivalent to calculating P_p from the *algebraic Riccati equation* [1]:

$$P_p = AP_pA^T + Q - AP_pC^T[CP_pC^T + R]^{-1}CP_pA^T. \tag{2.14}$$

From P_p, the stationary gain K_p can be calculated via

$$K_p = AP_pC^T[CP_pC^T + R]^{-1}. \tag{2.15}$$

With K_p known, the filter equations can be narrowed down to [1]

$$\hat{x}_{k|k} = \hat{x}_{k|k-1} + K_p(y_k - C\hat{x}_{k|k-1}). \tag{2.16}$$

The computational effort of a matrix inversion, which is made by the full filter equations in Eq. 2.9 - Eq. 2.13, is proportional to n^3, where n is the number of states in the system. This means that if the number of states is doubled, the computational effort increases by a factor of eight. Using Eq. 2.16, only multiplication and addition are used, where the computational time is proportional to n [4].

2.1.2 Fixed lag smoothing

To improve the estimates, the Kalman filter can be modified to include future measurements [1].

In *fixed lag smoothing*, one is willing to accept a time delay of m samples to improve the estimates. This is done by letting the estimate of x_k be based on the measurements up to y_{k+m}. The idea is to expand the state vector x to include delayed state vectors. This means that certain variables have to be modified. Therefore, introduce the following:

$$x_k^i = x_{k-i},\ i = 0, \ldots, m+1 \tag{2.17}$$

and the expanded state vector

$$\bar{x}_k = \begin{pmatrix} x_k^0 \\ x_k^1 \\ \vdots \\ x_k^{m+1} \end{pmatrix}. \tag{2.18}$$

The estimation of x_{k-m}, given observations up to y_k, is now given by $\hat{x}_{k+1|k}^{m+1}$, i.e. the last part of the extended state vector seen in Eq. 2.18. The modified system now has the form

$$\bar{x}_{k+1} = \bar{A}\bar{x}_k + Bu_k + \bar{w}_{1_k} \tag{2.19}$$
$$z_k = \bar{C}\bar{x}_k + Du_k + \bar{w}_{2_k}, \tag{2.20}$$

where

$$\bar{A} = \begin{pmatrix} A & 0 & 0 & \dots & 0 & 0 \\ I & 0 & 0 & \dots & 0 & 0 \\ 0 & I & 0 & \dots & 0 & 0 \\ 0 & 0 & I & \dots & 0 & 0 \\ \vdots & \vdots & \vdots & \ddots & \vdots & \vdots \\ 0 & 0 & 0 & \dots & I & 0 \end{pmatrix}, \tag{2.21}$$

$$Cov[\bar{w}_{1_k}] = \bar{Q} = \begin{pmatrix} Q & 0 & \dots & 0 \\ 0 & 0 & \dots & 0 \\ \vdots & \vdots & \ddots & \vdots \\ 0 & 0 & \dots & 0 \end{pmatrix}, \tag{2.22}$$

$$\bar{C} = \begin{pmatrix} C & 0 & \dots & 0 \end{pmatrix}. \tag{2.23}$$

Now estimations of $\hat{x}_{k-m|k}$, $\hat{x}_{k-m+1|k}$,...,$\hat{x}_{k|k}$ can be made by applying the Kalman filter to Eq. 2.19 - Eq. 2.20. This yields

$$\hat{\bar{x}}_{k+1|k} = \bar{A}\hat{\bar{x}}_{k|k-1} + \bar{K}_k(y_k - \bar{C}^T\hat{\bar{x}}_{k|k-1}) \tag{2.24}$$
$$\bar{K}_k = \bar{A}\bar{P}_{k|k-1}\bar{C}^T[\bar{C}\bar{P}_{k|k-1}\bar{C}^T + R]^{-1} \tag{2.25}$$
$$\bar{P}_{k+1|k} = \bar{A}\bar{P}_{k|k-1}\bar{A}^T + \bar{Q} - \bar{K}_k\bar{C}\bar{P}_{k|k-1}\bar{A}^T. \tag{2.26}$$

$\bar{P}_{k|k-1}(0,0)$ is acquired from the original, non-expanded system [1].

2.1.3 Observability

The Kalman filter is used to estimate the unknown states $\hat{x}_k$ from the measurements y_k. To accomplish this, there must be a strong coupling between

the state vector and the measurements. To measure if the coupling is strong enough, Eq. 2.27 is used.

$$O(A,C) = \begin{pmatrix} C \\ CA \\ CA^2 \\ \vdots \\ CA^{n-1} \end{pmatrix}, \tag{2.27}$$

where A and C are the matrices from the system and n the number of states. If the columns of the matrix O are linear independent, i.e. the matrix has full rank, the system is observable. Then, and only then, can all the states of the state vector x_k be estimated. An observable system also means that the estimation is unbiased and the covariance matrix non-singular.

Unfortunately, since O does not depend on Q and R, no information is given how good the filter is, i.e. the signal-to-noise ratio is not revealed with this method [1].

2.2 Vehicle dynamics

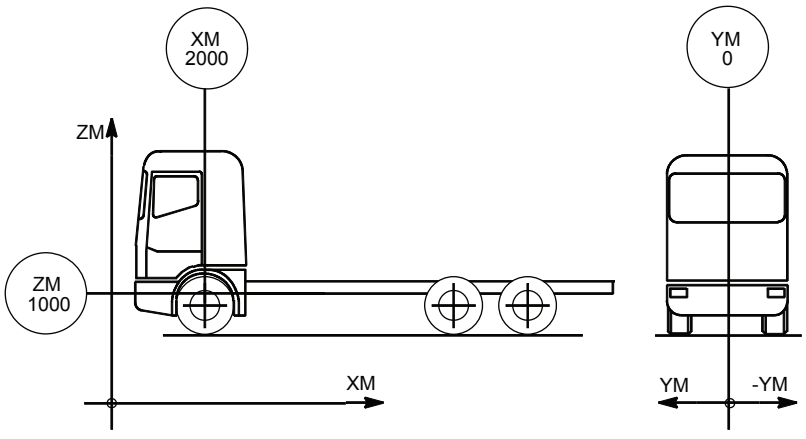

Figure 1: *The coordinate system of a truck. The measurements are in millimeters.*

For trucks, the complete chassis is the starting point for coordinate dimensioning. The origin is defined as follows [9]:

- The coordinate plane **XM0**, i.e. the plane where x = 0, is 2000 millimeters in front of the theoretical centre of the front axis. Coordinates to the right of this plane, which is backwards in the vehicle's driving direction, are positive. To the left of the plane, the coordinates are negative.

- The coordinate plane **YM0** is the theoretical centre between the frame side members. Coordinates to the right of the centre plane in the vehicle's direction of travel are positive. Coordinates to the left are negative.

- The coordinate plane **ZM0** is defined as 1000 millimeters below the lower edge of the frame side members. Coordinates above this 0-plane are positive, and the ones below are negative.

The axis are denoted with an M to separate the main coordinate system from the sub-coordinate systems. The sub-coordinate systems will not be regarded in this thesis, and the axis will from now on only be denoted X, Y and Z. An overview of the coordinate system can be seen in Fig. 1, where the measurements are in millimeters.

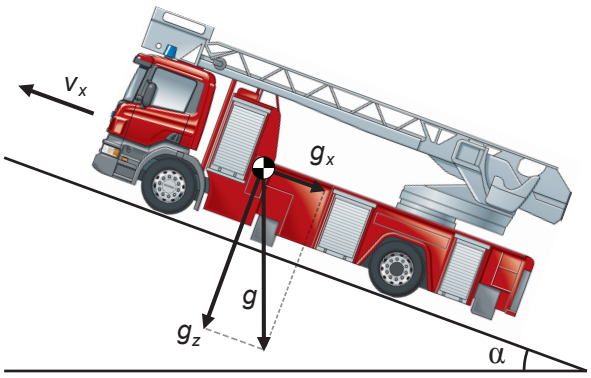

Figure 2: *One way of dividing the relevant accelerations acting on the truck. v_x corresponds to the velocity in the x-plane, α is the road slope angle, g the gravity, g_x the longitudinal gravity component and g_z the vertical gravity component.*

A truck traveling up, or down, a slope has different kinds of accelerations acting on it. A schematic simplified view of how the accelerations can be divided can be seen in Fig. 2. Also marked in the figure is the direction of the velocity in the x-plane. The longitudinal gravity component g_x is

calculated, and solved for the angle α_{rad}, as

$$g_x = g \cdot \sin(\alpha_{rad}) \Leftrightarrow \alpha_{rad} = \arcsin(\frac{g_x}{g}), \tag{2.28}$$

where g corresponds to the gravity.

As Fig. 2 suggests, the effects measured by a longitudinal accelerometer, a_{long}, will be the sum of the time-derivative of the velocity and the gravity component in x-direction. The effects are measured, and solved for g_x, as

$$a_{long} = \dot{v}_x + g_x \Leftrightarrow g_x = a_{long} - \dot{v}_x. \tag{2.29}$$

2.2.1 Pitch

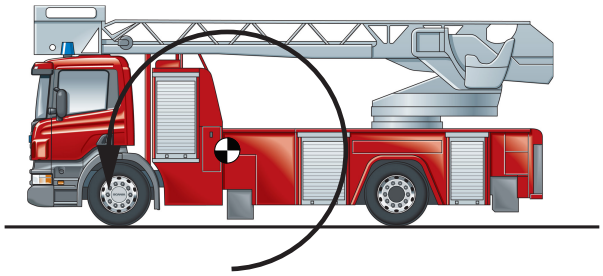

Figure 3: *The arrow shows how the pitch effects the truck.*

There is sometimes a difference between the road slope angle and the truck angle. The road slope angle, as well as the truck angle, can be defined as the deviation from the horizontal plane. The difference between the angles is called *pitch*. The pitch is denoted γ and measured in degrees. How the pitch affects the truck can be seen in Fig. 3. The pitch is mostly seen during powerful retardations, which causes the truck to *kneel* [12].

How much the truck pitches depends on many external parameters. Examples of such include the type of suspension and weight of the carriage as well as how powerful the retardation is. Many of these parameters change a lot when the truck is being used, e.g. weight, center of gravity, etc.

2.2.2 Centripetal acceleration in vertical curves

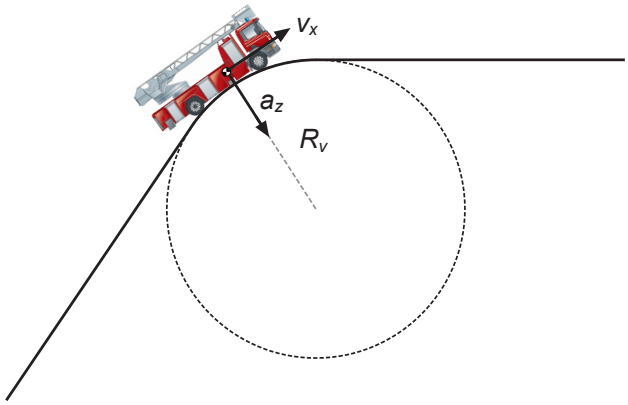

Figure 4: *Vertical centripetal acceleration on a vehicle in a vertical curve, where a_z is the vertical centripetal acceleration, v_x is the velocity of the vehicle and R_v is the radius of the vertical curve.*

The vertical curves before and after inclines, described in Section 2.4, give rise to a vertical acceleration on the vehicle. This vertical acceleration is generated from a centripetal force acting on the vehicle, as seen in Fig. 4.

In theory, this acceleration is perpendicular to the longitudinal accelerometer, of which the road slope is estimated from. Therefore, it should not influence the results of the road slope estimation. In practice, however, this might not be the case. Depending on the sensor position, there might be a small contribution from the vertical acceleration caught by the longitudinal accelerometer. This contribution is, however, very hard to distinguish.

The centripetal acceleration caused by the vertical curves is calculated as

$$a_z = \frac{v_x^2}{R_v}, \tag{2.30}$$

where a_z is the vertical centripetal acceleration, v_x is the velocity of the truck and R_v the radius of the vertical turn [10].

2.2.3 Centripetal acceleration in horizontal curves

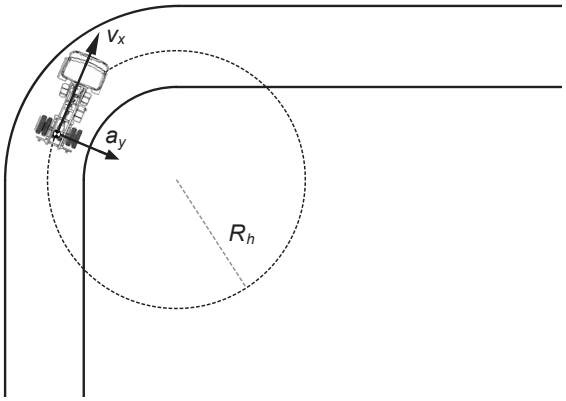

Figure 5: *Horizontal centripetal acceleration on a vehicle, viewed from above, in a horizontal curve, where a_y is the horizontal centripetal acceleration, v_x is the velocity of the vehicle and R_h is the radius of the horizontal curve.*

Just as in the vertical curves, there is a centripetal acceleration generated in the horizontal turns. This acceleration is directed inwards the turn, i.e. in the lateral direction, as seen in Fig. 5. Therefore, this acceleration is also perpendicular to the longitudinal accelerometer.

This acceleration is calculated as

$$a_y = \frac{v_x^2}{R_h}, \tag{2.31}$$

where a_y is the horizontal centripetal acceleration, v_x is the velocity of the truck and R_h the radius of the horizontal turn [10].

2.3 Properties of the trucks used

The previous section described vehicle dynamics in general, but all trucks have their individual properties. These properties depend, for example, on what kind of suspension the truck has, the wheel configuration as well as the weight of the truck.

To be able to develop a model that can be used for all kinds of trucks, two different kinds were used during the collecting of data. The trucks were chosen to have as different properties as possible in order to develop a model that fits them both. The properties of these trucks are explained in this section.

2.3.1 Electra

Figure 6: *Picture of Electra. Courtesy of Lars Holmlund, Scania CV AB.*

Electra is a 560 horse power tractor with air suspension. A picture of Electra can be seen in Fig. 6. It has a 4x2 wheel configuration and an axis distance of 3550 millimeters. 4x2 is a way of describing the wheel configuration of a truck. The 4 corresponds to that the truck has four wheels and the 2 represents that the two rear ones are driven. A schematic view of the wheel configuration of Electra can be seen in Fig. 7, where the black wheels correspond to the driven ones. Also marked in the figure is the approximate position of the longitudinal accelerometer used in this thesis.

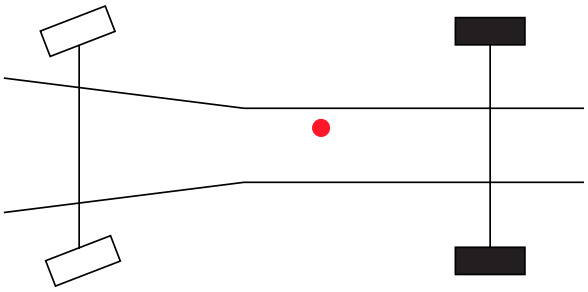

Figure 7: *The wheel configuration of the 4x2 tractor Electra, with the sensor position marked in red and the driven wheels in black.*

This type of suspension is controlled via valves and pumps to make the

vehicle stay as horizontal as possible when driven. For longer inclines, this may cause some problem since it is assumed that the truck angle equals the road slope angle, explained in Section 3.2.1. If the vehicle angle is changed, the road slope estimation will be incorrect [15]. This might have influenced the results in this thesis. The problem is elaborated in Section 5.1.

The air suspension system updates, and corrects the angle of the truck, once every 60 seconds. This means that if the update happens in an incline the road slope angle estimation the following 60 seconds might be inaccurate [15].

2.3.2 Mustang

Figure 8: *Picture of Mustang.*

Mustang, seen in Fig. 8, is a container carrying truck with a 6x4 wheel configuration and 420 horse power. This wheel configuration corresponds to that the truck has six wheels, and the four rearmost are driven. A schematic view of the wheel configuration, as well as the frame side members, can be seen in Fig. 9, where the sensor position is marked in red and the driven wheels are marked in black.

This truck has steel suspension and an axis distance of 3900 millimeters. The steel suspension, as well as the greater axis distance, mean that it is less prone to pitch than Electra. This is due to the fact that a truck with steel suspension is more stiff than a truck with air suspension [15].

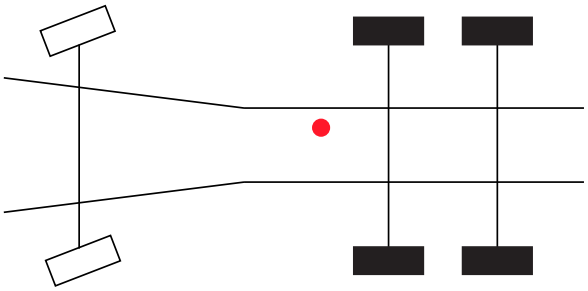

Figure 9: *The wheel configuration of the 6x4 truck Mustang, with the sensor position marked in red and the driven wheels in black.*

2.4 How roads are built

The information given in this section is based on the information provided by *Vägverket*. *Vägverket*, national road administration, is a public authority in Sweden in charge of planning, building and maintenance of all public roads in Sweden [5]. The information given and standards cited may vary from other countries. For more information on roads in Sweden, please see [6] and [7].

Roads are built with a constant incline. Between the constant inclines, convex and concave vertical curves with a constant radius, are fit to obtain a smooth transition. The inclines and vertical curves are adjusted to match the height of the surrounding terrain. The incline is measured in % and uses the horisontal plane as reference, where the angle is 0 %. The incline is negative in a downward slope.

Before a road is built and the road slope angle is decided, many aspects are taken into consideration [6]:

- Traffic safety
- Velocity and capacity
- Vehicle effects
- Dynamics of driving
- Terrain adjustment
- Esthetics

The total height of a slope, without longer so called *resting planes*, is critical for vehicle effect and travel time, and not the individual size of the combination concave vertical curve - incline - convex vertical curve. A resting plane is a part of the slope where the incline is less, or almost flat, so that the vehicle has a chance to regain its speed to overcome the next incline. See Fig. 10 for explanation of the resting plane.

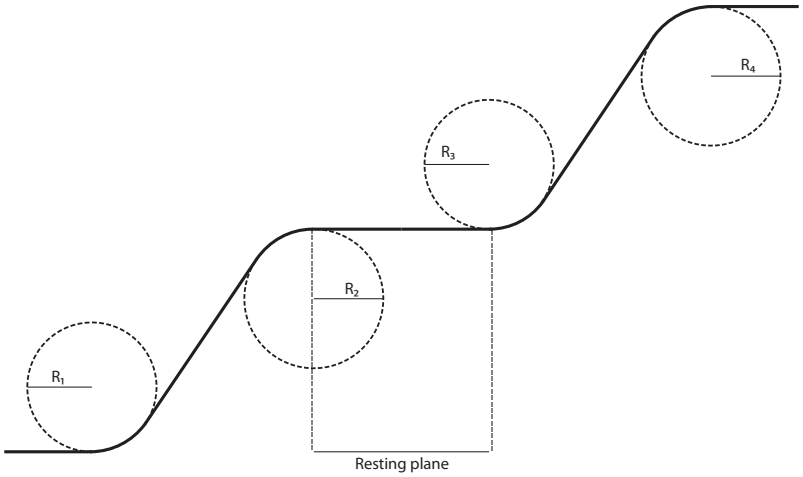

Figure 10: *Explanation of resting plane, which is the flat part between the inclines.* R_1 *-* R_4 *represent the radii of the vertical curves.*

The maximum incline for a countryside road in Sweden is chosen so that a heavy duty vehicle can overcome its starting resistance without too much effort. Good standard in Sweden is 6 %. In the conurbation areas, the roads' incline is decided with vehicles trafficability and safety in mind. Conditions of the slope may vary, e.g. with weather. Road slope angles over 10 % cause large difficulties of both accelerating and decelerating during winter road conditions. Therefore, roads which include inclines larger than 10 %, are recommended to have an alternate route. More standardized inclines for different road types can be seen in Table 1.

Line of sight is also an important aspect to consider when planning a road, but this part will not be covered in this thesis. Since there is a large difference in line of sight for a passenger car and a long haul vehicle, both are taken into consideration.

	Good standard	Less good standard	Low standard
Countryside	6 %	7 %	8 %
Intersection, conurbation	2,5 %	3,5 %	9 %
Stretch, conurbation	6 %	8 %	9 %

Table 1: *Maximum longitudinal road slope angle.*

2.4.1 Deciding the radius for the vertical curves

When the radius of a vertical curve is to be chosen, not only the surrounding terrain and traffic safety are taken into consideration. Driver and passenger comfort are also an important aspect. *Vägverket* uses Table 2 to decide an appropriate radius for the vertical curves, based on the vertical acceleration of the vehicle [7].

The vertical acceleration is caused by the centripetal force acting on the vehicle. The centripetal force is perpendicular to the road, directed toward the rotation point, as described in Section 2.2.2.

Standard	Vertical acceleration	Remark
Good	0 - 0.5 m/s^2	No discomfort
Less good	0.5 - 1.0 m/s^2	Some discomfort

Table 2: *Maximum vertical acceleration in vertical curves.*

The vertical acceleration of a vehicle caused by the vertical curves is calculated from Eq. 2.30 in Section 2.2.2. To illustrate this, consider the following simple example:

To achieve good standard on a Swedish highway, so that the passengers do not experience any discomfort in the vertical curves due to vertical acceleration, the acceleration must not exceed 0.5 m/s^2 according to Table 2. The speed limit on Swedish highway is 110 km/h, i.e. 30.5 m/s. With that knowledge in mind, the radius of the vertical curves can be calculated to be at least 1860 meters. The calculations for the example are

$$a_z = \frac{v_x^2}{R_v} \Rightarrow R_v = \frac{v_x^2}{a_z} = \frac{30.5^2}{0.5} = 1860 \text{ meters.}$$

Note that these standards are set with regards to personal cars in this case, trucks have a speed limit of 90 km/h on Swedish highways. Therefore, they experience less vertical acceleration.

3 Method

This chapter describes how the estimations are made. The chapter starts with an explanation of how the data was collected. How the model was developed is explained in the following section. The last section of the chapter explains how the Kalman filter was designed.

3.1 Collecting the data

First of all, data must be collected for analysis in Matlab. As further explained in Section 2.3, the data was collected in two different kinds of trucks to be able to distinguish differences and similarities between the two. To be able to make a comparison between them, the driving had to be done in the same way. However, this was not always possible due to other traffic on the test course.

By standing still in a flat part of the test course, data was collected for the purpose of calibrating. By using this as a zero-level, it was made sure that the signals would not have an stationary offset.

Since it was not yet decided how the model would be constructed and what properties would be taken into consideration, all signals in the trucks were measured and saved, in all driving scenarios. The signals used are sampled with 25 Hz.

The data was collected by driving a series of tests. Both specific tests to try the sensor's robustness and tests that would simulate real driving, i.e. how the trucks are used in every day life. The tests driven can be seen below.

- 16 % incline
- 18-20 % incline
- Real driving simulation on test course
- Powerful retardation
- Horizontal turns

To be certain that the estimation in the inclines were accurate, the tests were performed several times. The speed of the sensor was put to test by driving up the slopes in 25 km/h, and one test for comparison driven in 5 km/h. Also, the sensor's robustness was tested by both accelerating up the slopes and with a stop and start in the middle of the slopes. All four of these tests, seen below, were carried out in both inclines available, one with an incline of 16 % and one with 18-20 %.

- 25 km/h
- 5 km/h
- Acceleration
- Stop and start

An additional accelerometer was installed to measure vertical acceleration. The purpose of this accelerometer was to calculate the road slope angle from it and use it as validation for the estimations obtained from the longitudinal accelerometer. Unfortunately, this was not possible. The reason is described in Section 6.2.

In some retardations tests, an external sensor to measure pitch was installed. This sensor was used to determine the influence of pitch on the road slope estimation.

3.1.1 Low-pass filtering the signals

To get rid of high frequency noise, generated mainly from the engine of the truck, the signals often pass through a low-pass filter before an estimation can begin.

A Butterworth filter was constructed for this purpose, but was later removed. The filter was removed since the real-time model must be capable of handling unfiltered signals in order to have a faster response-time.

The Kalman filter has low-pass filter properties in the terms of removing the noise of the input signals in order to generate noise-free estimations.

3.2 Road slope model

This section describes the road slope model used for the estimations.

3.2.1 Simplifications

To make sure that the obtained estimation would not have an stationary offset, the signal from the accelerometer has to be calibrated. In this thesis, this is done by letting the vehicle stand still on flat ground and sampling the signal from the longitudinal accelerometer. By subtracting the mean of this signal from the signal from the other driving scenarios before the estimation is made, one can be certain that the estimation has a correct zero-level.

Even though this is a large simplification, it is assumed that the truck angle equals the road slope angle, i.e. the pitch equals zero. How the pitch

affects the truck was described in Section 2.2.1. In the sequel, the road slope angle will be assumed to be equal to the truck angle, and will be denoted α.

In the vertical curves, explained in Section 2.4, the vehicle is subject to a vertical acceleration. How the vertical acceleration effects the vehicle is described in Section 2.2.2. In this thesis, the vertical acceleration is assumed to be perpendicular to the longitudinal acceleration, and therefore does not have any influence on the signal from the accelerometer used for the estimation of road slope angle.

The horizontal curves also create a centripetal acceleration acting on the vehicle. Just as the centripetal acceleration generated from the vertical curves, this acceleration is assumed to be perpendicular to the longitudinal accelerometer and therefore, does not influence the results of the road slope angle estimation.

3.2.2 Dividing up the forces

A possible way of dividing the forces of the truck in a slope was presented in Section 2.2. As can be seen in Eq. 2.29, one can solve for g_x by subtracting the change in velocity, $\dot{v}$, from the signal from the longitudinal accelerometer. The correlation between the resulting signal, g_x, and the wanted road slope angle α can be seen in Eq. 2.28. It can be seen that by dividing with the gravity constant g and then use the non-linear function *arcsine*, one can solve for α, which is in radians.

$$a_{long} = \dot{v} + g_x \Leftrightarrow g_x = a_{long} - \dot{v}$$
$$g_x = g \cdot \sin(\alpha_{rad}) \Leftrightarrow \alpha_{rad} = \arcsin(\frac{g_x}{g})$$

In Eq. 2.28, the angle α is presented in radians. As described in Section 2.4, the unit traditionally used for inclines is %. Eq. 3.1 shows how the translation from radians to % is done, where the relation from Eq. 2.28 is used. From now on, α will be presented in %.

$$\alpha_{\%} = 100 \cdot \tan(\alpha_{rad}) = 100 \cdot \tan(\arcsin(\frac{g_x}{g})) \tag{3.1}$$

3.2.3 Initial thoughts

Many different states were considered for the model. What states could contribute to an accurate estimation of the road slope angle, without being too computationally demanding?

It was clear that the vehicle acceleration $\dot{v}$ had a large influence on the signal from the longitudinal accelerometer and a strong coupling with the velocity v. Therefore, the choice to have both $\dot{v}$ and v as states was given.

The angle α was thought of as a state, but this idea was later discarded. The state would introduce non-linearities to the system, which would imply that an Extended Kalman filter was needed. By choosing g_x as a state instead, a traditional Kalman filter could be used, where calculations can be made offline, and less computational power is required for the filter in the real-time application.

The thought of g_z as a state was also discussed, but discarded due to the non-linear properties of the *cosine* function. This is further elaborated in Section 6.2. By using g_x instead, the non-linear function involved is *sine*, which is more beneficial. The properties of *sine* is also discussed in Section 6.2.

To include the lateral gravity component, g_y, was also considered. The idea was to estimate the lateral road slope angle as well. After analysis of the signal from a lateral accelerometer, the idea was discarded. The reason is that the centripetal acceleration in a horizontal turn is too high, ~ 3 m/s^2, compared to the lateral angle wanted, ~ 4 % [6]. Therefore, the angle is too hard to distinguish from the acceleration.

The time-derivative of the longitudinal gravity component, $\dot{g}_x$, was also considered as a state. The idea was to be able to identify when a vehicle had passed the incline, and the road started to get horizontal again. The thought was discarded for computational improvement[1] and lack of area of application. However, the model can easily be extended to include that state.

3.2.4 The final model

The states chosen for the model are vehicle acceleration $\dot{v}$, vehicle velocity v and the longitudinal gravity component g_x. The final model can be seen in Eq. 3.2 - Eq. 3.3, where an *Euler approximation* is used to obtain the derivative of the velocity. T represents the sampling interval.

$$\begin{pmatrix} \dot{v}_{k+1} \\ v_{k+1} \\ g_{x_{k+1}} \end{pmatrix} = \begin{pmatrix} 1 & 0 & 0 \\ T & 1 & 0 \\ 0 & 0 & 1 \end{pmatrix} \begin{pmatrix} \dot{v}_k \\ v_k \\ g_{x_k} \end{pmatrix} + \begin{pmatrix} T^2/2 & 0 \\ T & 0 \\ 0 & T \end{pmatrix} \begin{pmatrix} \ddot{v}_k \\ \dot{\epsilon}_k \end{pmatrix} \tag{3.2}$$

$$\begin{pmatrix} v_k \\ a_{long_k} \end{pmatrix} = \begin{pmatrix} T & 1 & 0 \\ 1 & 0 & 1 \end{pmatrix} \begin{pmatrix} \dot{v}_k \\ v_k \\ g_{x_k} \end{pmatrix} + w_{2_k} \tag{3.3}$$

The input signals, $\ddot{v}$ and $\dot{\epsilon}$, are modeled as white noise. This is a common way of modeling uncertainties, since it allows the signals to do random walks,

[1] The computational effort of a filter, where calculations are made online, increases proportional to n^3, where n is the number of states [4]. Therefore, it is important only to use the necessary states.

which can not be predicted [1].

The Euler approximation is a way of calculating the time-derivative of a signal, e.g. acceleration from velocity, which is used in this thesis. The Euler approximation used is

$$\dot{v}_k = \frac{v_{k+1} - v_k}{T} \Leftrightarrow v_{k+1} = T \cdot \dot{v}_k + v_k. \tag{3.4}$$

By using Eq. 2.27 in Section 2.1.3, the system can be showed to be observable.

3.3 Designing the Kalman filter

As described in Section 2.1, the parameters of the Kalman filter have to be decided with the system's properties in mind. The parameters to be determined are the covariance matrices Q and R, as well as the initial values of the error covariance matrix P and the state vector x, denoted P_0 and x_0, respectively.

3.3.1 The Kalman filter

The Kalman filter used in this thesis is linear and discrete in time. The covariance matrices are here assumed to be constant and simply be denoted Q and R.

3.3.2 Covariances matrices

Also explained in Section 2.1 are the properties of Q and R compared to each other. When designing a Kalman filter, a compromise between a fast, but noise sensitive, filter and a noise proof, but slow, filter has to be made.

The elements are adjusted so that the estimations are satisfying in all driving scenarios. Therefore, a compromise is made between obtaining a fast filter, for the incline tests, and a robust filter, which is appropriate in the retardation scenarios.

To calculate the variances of the process noise covariance matrix Q, the signals are analyzed visually. Then, with some calculations, it was possible to estimate in which range the states could change from one sample to the next. Knowing the range of the elements for the matrix, the values are tuned to obtain a good estimation. Therefore, the values used in the matrix differ slightly from the calculated ones.

The variance of the vehicle acceleration $\sigma_{\dot{v}}$ is decided by looking at the steepest gradient of the acceleration signal during a powerful acceleration. The variance was found to be about 0.5.

The maximum acceleration for a tractor, equipped with the large V8 of 620 horse power, without trailer, is approximately 0.3 g [11]. This is equivalent to an acceleration of about 3 m/s^2. Since the signals are sampled with a frequency of 25 Hz, this acceleration corresponds to a variance for the velocity of $\sigma_v = \frac{3}{25} = 0.12$. Different values of this variance were calculated and tested, also with regard to the maximum retardation, which is approximately 6 m/s^2 [11].

The calculation of the variance for g_x is a bit more complicated. A reasonable slope in every day driving can be considered to be less than 10 %, as explained in Section 2.4. A 10 % incline corresponds to $g_x = 1$ m/s^2, or $\alpha_{rad} = 0.1$ radians, which can be seen by solving for g_x, or α_{rad}, in Eq. 3.1. A truck is allowed to drive 90 km/h, which corresponds to 25 m/s. Imagine that a truck is going up a 10 % slope at that speed, then a concave vertical curve is used for a transition to a flat road, which means that g_x changes from 1 m/s^2 to 0 m/s^2. As explained in Section 2.4.1, the vertical curve can have a radius of 1860 meters and still maintain good standard. If the angle of the slope, α, is 0.1 radians, and the radius is 1860 meters, the part on the circumference where the road is translates to 186 meters. If truck has a velocity of 25 m/s, the distance 186 meters will take 7.4 seconds. Therefore, change in g_x in the vertical curve is $1 - 0 = 1$ m/s^2 on 7.4 seconds, which is 0.135 m/s^3. By dividing this value with the sampling frequency, the variance is obtained as $\sigma_{g_x} = 0.0054$. Here it is assumed that the decrease in acceleration is linear. The matrix used in the thesis is

$$Q = \begin{pmatrix} \sigma_{\dot{v}} & 0 & 0 \\ 0 & \sigma_v & 0 \\ 0 & 0 & \sigma_{g_x} \end{pmatrix} = \begin{pmatrix} 0.3 & 0 & 0 \\ 0 & 0.005 & 0 \\ 0 & 0 & 0.003 \end{pmatrix}. \tag{3.5}$$

To determine the covariance matrix R, a high-pass filter is used. By high-pass filtering the signals, the measurement noise can be analyzed to know in what range it appears. With a high-pass filter, the lower frequency behavior is removed and only the high frequency noise is left. By using this technique, and some tuning,

$$R = \begin{pmatrix} \sigma_{a_{long}} & 0 \\ 0 & \sigma_v \end{pmatrix} = \begin{pmatrix} 0.5 & 0 \\ 0 & 0.3 \end{pmatrix}, \tag{3.6}$$

was obtained.

3.3.3 Initial values

Many of the test drives are short, some of them only 10-20 seconds long. To avoid that any initial transients interfere with the estimation, the real starting values from the vectors containing the signals are used as initial values for the states estimating the acceleration and the velocity. The acceleration vector used here are calculated via Euler approximation from the velocity. The starting value of g_x is set to zero, i.e. it is assumed that the vehicle is horizontal at the beginning of each test drive. This assumption is not always true, but the estimation quickly converges to a correct value, without transient behavior.

Since it is known that the initial values are correct, the initial values in the error covariance matrix P_0 are designed with that in mind. The elements of the matrix is small, which means that there is a large trust in the initial values. For more information regarding this theory, see [1].

3.3.4 Varying covariance matrix Q

During powerful retardations, in order to increase the accuracy of the estimations, the covariance matrix Q can be changed. By changing the values in the matrix, the system response and the estimations are slowed down. A brake scenario can be detected by looking at the brake pedal position. When the brake pedal is pushed to more than 25 % of its full position, the matrix is changed. The new values of the matrix, which is now called Q_{bpp}, are

$$Q_{bpp} = \begin{pmatrix} 10 & 0 & 0 \\ 0 & 10 & 0 \\ 0 & 0 & 0.1 \end{pmatrix} \cdot Q, \tag{3.7}$$

where Q is the original covariance matrix, presented in Eq. 3.5.

By changing the matrix, the acceleration and the velocity are allowed to change but the last state, g_x, is not. By punishing that state, and allowing the other states to drift away, the incline estimation is less sensitive to changes.

4 Results

This chapter is divided into four sections. First are the results obtained from the tests in the inclines presented, followed by the results in a few brake scenarios. In the next section, the effects of horizontal centripetal acceleration are laid out. Results of the estimations of a few laps on the test course are presented in the following section. These test drives are meant to simulate real driving, for the purpose of investigating of how the estimation would work in real traffic. The chapter is then concluded with a section where the estimations are compared to GPS-data.

In the scenarios where it is considered necessary, both the results obtained with Kalman filter and fixed lag smoothing are shown. Where fixed lag smoothing is shown, only the road slope estimations with various delays are presented. The other states are irrelevant in these sections.

Where possible, a comparison between Mustang and Electra is made.

Analysis showed that the velocity estimate did not differ from the measured signal. Therefore, it is chosen to present only the estimations for the different driving scenarios, and not the measured signals.

4.1 Inclines

In this section, the behavior of the estimations in the inclines are presented. The section starts with presenting the estimations made with the Kalman filter, followed by the estimations obtained when the fixed lag smoothing is applied.

4.1.1 Kalman filtering

Here are the estimations made with the Kalman filter presented. First, the tests carried out in the 16 % incline case are shown, followed by the tests done in the 18-20 % incline case.

For easier comparison of the tests done in the respective case, the estimations are also presented as functions of distance, instead of time.

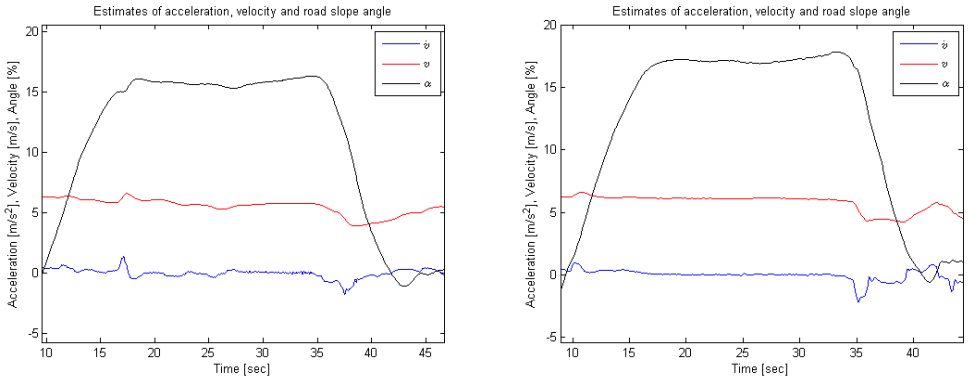

(a) *Mustang* **(b)** *Electra*

Figure 11: *The results obtained from a test in the 16 % incline carried out at 25 km/h. The blue curves show the estimated accelerations, the red curves the estimated velocities and the black curves show the estimated inclines. The curves are shown as functions of time.*

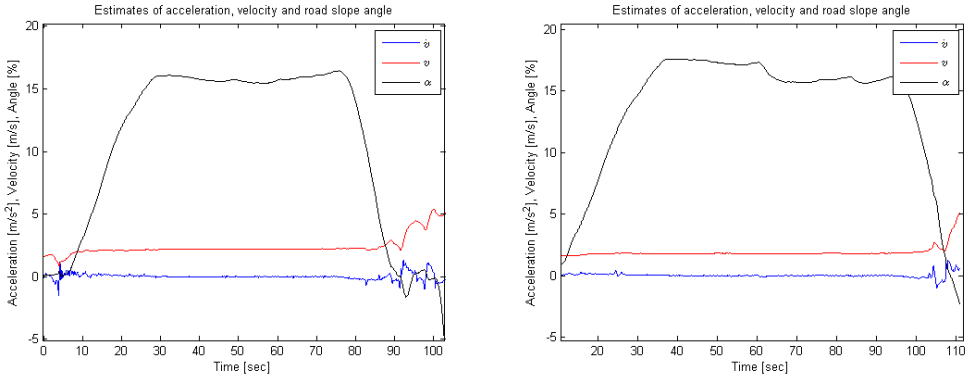

(a) *Mustang* **(b)** *Electra*

Figure 12: *The results obtained from a test in the 16 % incline carried out at 5 km/h. The blue curves show the estimated accelerations, the red curves the estimated velocities and the black curves show the estimated inclines. The curves are shown as functions of time.*

Fig. 11 and Fig. 12 show the 16 % incline case at constant velocity. The velocities are 25 km/h and 5 km/h, respectively.

In Fig. 12b, Electra shows an offset behavior after 60 seconds. The reason

for this could be that the suspension system updates, and corrects, the angle of the truck. Therefore, the road slope angle estimation is also affected.

Seen especially in Fig. 12b and Fig. 11a is a slight increase in the road slope estimation before the estimation drops to 0 %. The increases are seen at 35 and 80 seconds, respectively. This phenomenon could be due to vertical centripetal acceleration caused by the vertical curves, but it is not certain. It could also be that the incline is a bit steeper at the end.

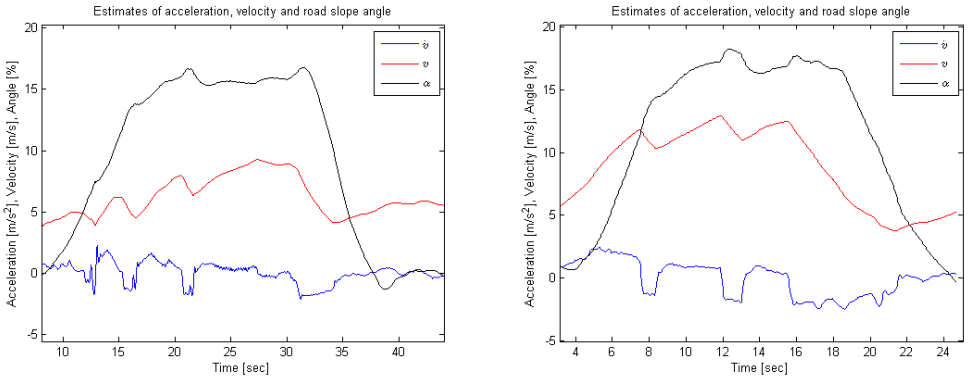

(a) *Mustang* **(b)** *Electra*

Figure 13: *The results obtained from a test accelerating up the 16 % incline. The blue curves show the estimated accelerations, the red curves the estimated velocities and the black curves show the estimated inclines. The curves are shown as functions of time.*

In Fig. 13, the system is tested by accelerating up the 16 % slope. It can be seen that Electra, in Fig. 13b, has a higher velocity than Mustang, in Fig. 13a. Since the acceleration is fairly equal, this should not influence the comparison.

The road slope estimations are not as smooth as when the velocities are kept constant. This tests show that the acceleration has an impact on the road slope estimation.

The increase at 33 seconds in Fig. 13a is probably due to the vehicle acceleration, not the reasons state above, i.e. vertical centripetal acceleration and steeper incline.

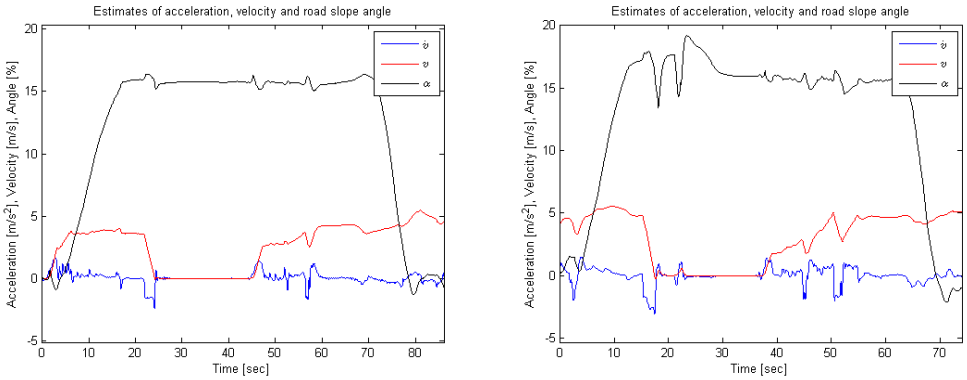

(a) *Mustang* **(b)** *Electra*

Figure 14: *The results obtained from a test in the 16 % incline with a stop and start. The stop takes place at 25 and 18 seconds, respecitvely. The vehicles are still for about 20 seconds. The blue curves show the estimated accelerations, the red curves the estimated velocities and the black curves show the estimated inclines. The curves are shown as functions of time.*

Fig. 14 shows a test drive in the 16 % incline case, with a stop and a start in the slope. It can be seen that the velocities and accelerations are zero for about 20 seconds. This test is executed in order to investigate the robustness of the system. Noticeable is the road slope estimation's oscillating behavior in the moment of retardation in Fig. 14b. The estimation is very inaccurate between 15 and 20 seconds, probably due to that the tractor is pitching.

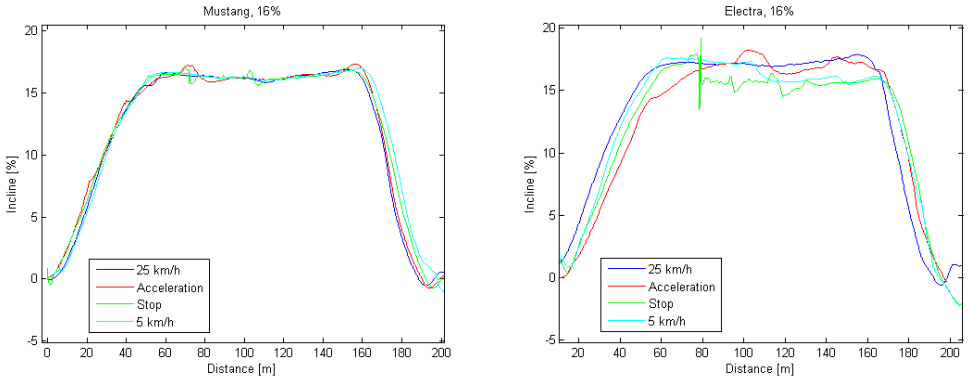

(a) *Mustang* **(b)** *Electra*

Figure 15: *Four test drives in a 16 % slope as functions of distance. The blue curves show the tests done in 25 km/h, the red ones the accelerating tests, the green ones show the tests with a stop and a start in the incline and the cyan colored curves show the incline at a velocity of 5 km/h.*

For easier comparison between the different test drives in the 16 % incline case, Fig. 15 shows the four test drives carried out in the 16 % slope as a function of distance. The distance is calculated from the velocity.

The road slope estimations in Fig. 15a show that the tests carried out in the 16 % incline with Mustang are very accurate. The estimations shown in Fig. 15b are not as equal. There is a difference between the estimations obtained with Electra. Especially the acceleration test, shown by the red curve, and the stop test, the green curve, stands out. There is a bit of offset in the stop test from about 80 meters and forward, perhaps due to an update of the suspension system.

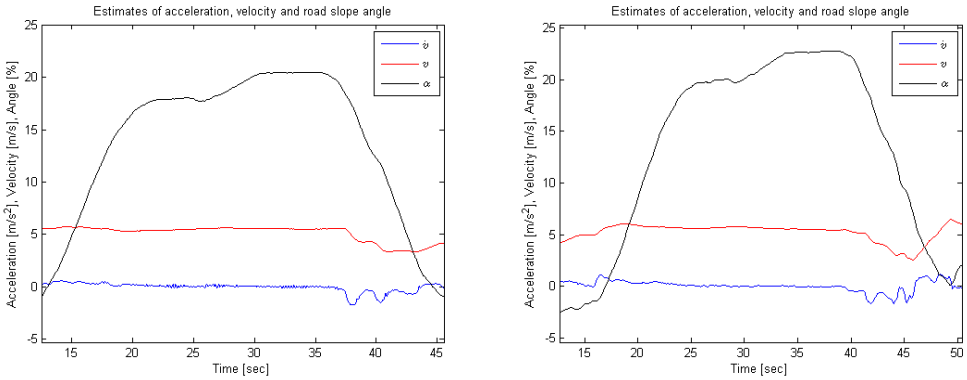

(a) *Mustang* **(b)** *Electra*

Figure 16: *The results obtained from a test in the 18-20 % incline carried out at 25 km/h. The blue curves show the estimated accelerations, the red ones the estimated velocities and the black curves show the estimated inclines. The curves are shown as functions of time.*

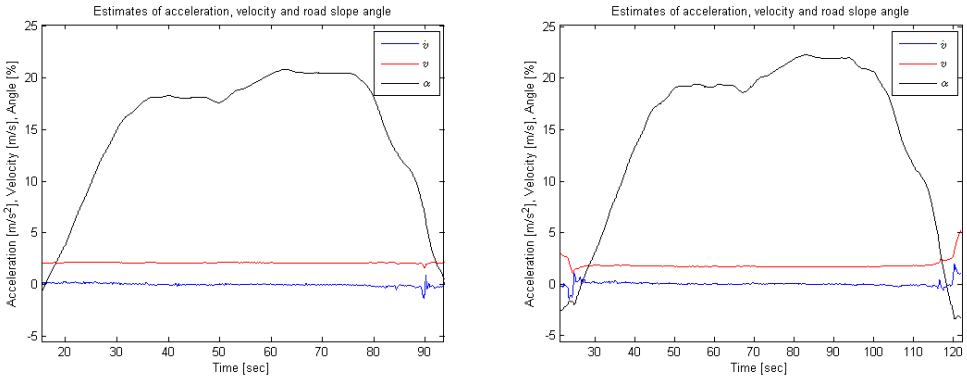

(a) *Mustang* **(b)** *Electra*

Figure 17: *The results obtained from a test in the 18-20 % incline carried out at 5 km/h. The blue curves show the estimated accelerations, the red ones the estimated velocities and the black curves show the estimated inclines. The curves are shown as functions of time.*

The 18-20 % incline case at constant velocities is shown in Fig. 16 and Fig. 17. The velocities are 25 km/h and 5 km/h, respectively.

These tests show very similar behavior, regardless of velocity. It can be seen that the road slope estimations are consistently higher with Electra,

than with Mustang. This may be because of the air suspension on Electra, which makes it more prone to pitch.

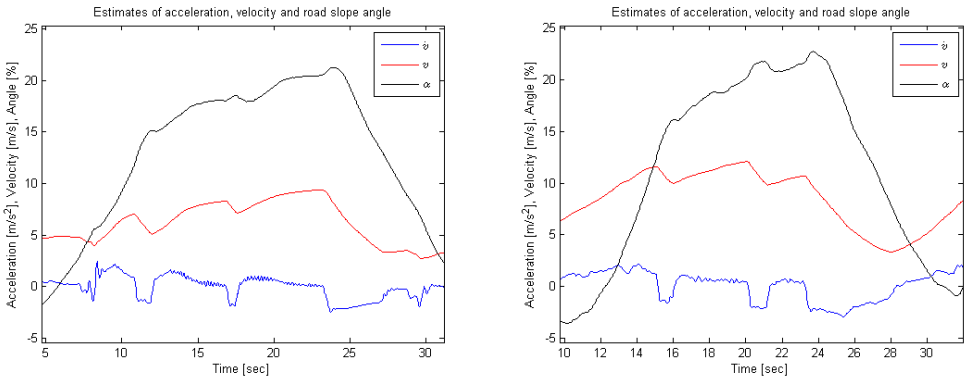

(a) *Mustang* **(b)** *Electra*

Figure 18: *The results obtained from a test accelerating up the 18-20 % incline. The blue curves show the estimated accelerations, the red ones the estimated velocities and the black curves show the estimated inclines. The curves are shown as functions of time.*

Fig. 18 shows the accelerating test in the 18-20 % incline. Just as in the same scenario in the 16 % incline, the velocity of Electra, in Fig. 18b, is slightly higher than with Mustang, in Fig. 18a.

The road slope estimations in Fig. 18 show some peaks during the acceleration, and the curves are not as smooth as when the velocities are kept constant. This is probably due to the elements of the covariance matrix, which are adjusted to obtain a good estimation in all driving scenarios. This mean that a compromise had to be made. By tuning the elements to obtain better results in these scenarios, other driving scenarios, e.g. the retardations, had gotten worse results.

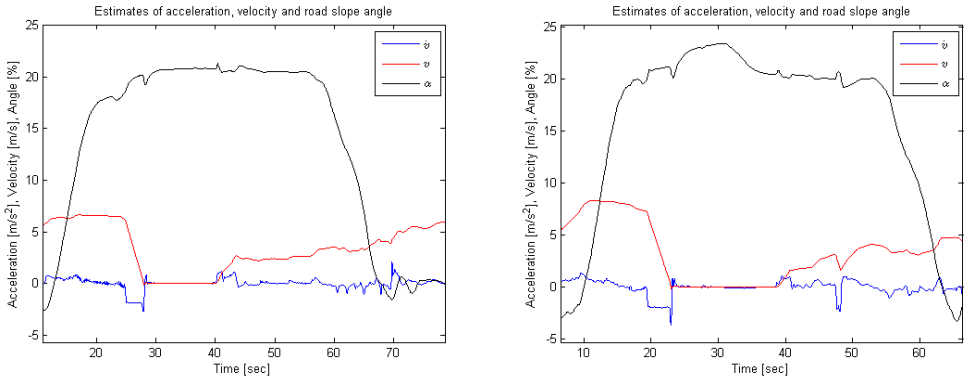

(a) *Mustang* **(b)** *Electra*

Figure 19: *The results obtained from a test in the 18-20 % incline with a stop and start. The stop takes place at 28 and 24 seconds, respectively. The start takes place at 40 and 38 seconds, respectively. The blue curves show the estimated accelerations, the red ones the estimated velocities and the black curves show the estimated inclines. The curves are shown as functions of time.*

In Fig. 19, the test with a stop in the 18-20 % incline is shown. The road slope angle estimations, showed in black, have lost its characteristic shape, seen in Fig. 16 and Fig. 17. This is due to the fact that the stops, which lasted about 12 and 14 seconds, respecively, took place in the 20 % part of the slope. As the curves are plotted against time, the curves are a bit miss-shaped since more time is spent in the 20 % part.

In Fig. 19b, a suspension update probably takes place after 30 seconds. This happens even though the velocity and the acceleration are kept at zero. The road slope estimation decreases to 20 %, which is the correct incline according to the available data. By looking at the previously shown results with Electra, the estimations are consistently higher than that.

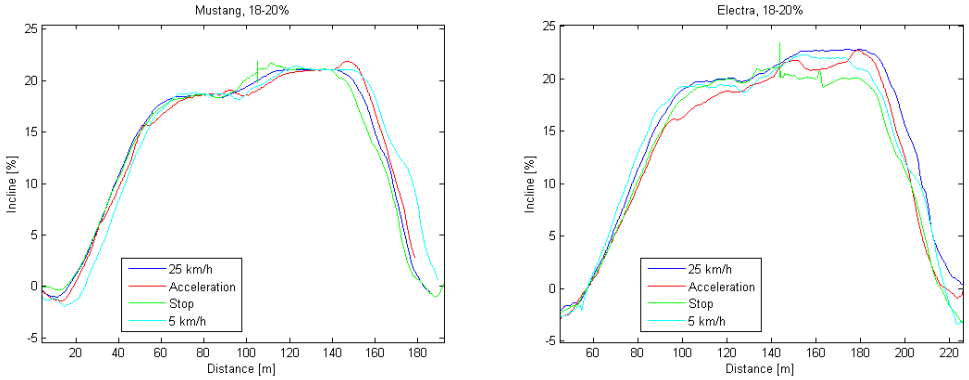

(a) *Mustang* **(b)** *Electra*

Figure 20: *Four test drives in the 18-20 % incline as functions of distance. The blue curves show the tests done in 25 km/h, the red ones the accelerating tests, the green ones show the tests with a stop and a start in the incline and the cyan colored curves show the incline at a velocity of 5 km/h.*

In the same way Fig. 15 shows the test drives in the 16 % incline, Fig. 20 shows the test drives carried out in the slope that increases from 18 % to 20 %. The figure shows incline as a function of distance, where the distance is integrated from the velocity.

As in the tests in the 16 % incline, Mustang shows consistency in the road slope estimates. The results obtained with Electra differs a bit more.

4.1.2 Fixed lag smoothing

Comparison between fixed lag smoothing and real-time estimation in the inclines is made in this section. The tough scenarios, i.e. the acceleration and the stop and start, are chosen for further investigation here. It is in these scenarios the largest gain can be obtained from the fixed lag smoothing.

The test drives are shown with 0, 1, 2 and 5 seconds delay of the road slope estimation, as functions of time. The other states, i.e. the vehicle acceleration and velocity, are not shown.

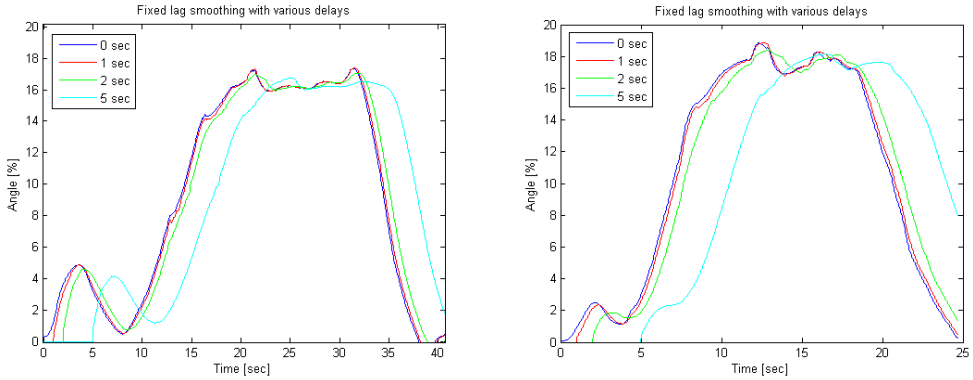

(a) *Mustang* **(b)** *Electra*

Figure 21: *Fixed lag smoothing in the 16 % incline, accelerating up the slope. The blue curves represent the Kalman filter estimation, i.e. without any delay. The red, green and cyan curves show the fixed lag smoothing with 1, 2 and 5 seconds delay, respectively. The curves are shown as functions of time.*

Fixed lag smoothing from the accelerating test showed in Fig. 13 is presented in Fig. 21. The improvements grow slightly as the delay increases.

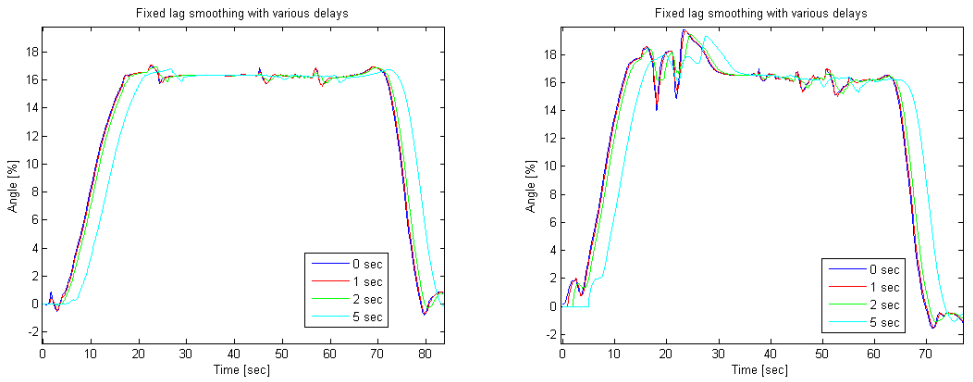

(a) *Mustang* **(b)** *Electra*

Figure 22: *Fixed lag smoothing in the 16 % incline, with a stop and a start in the slope. The blue curves represent the Kalman filter estimation, i.e. without any delay. The red, green and cyan curves show the fixed lag smoothing with 1, 2 and 5 seconds delay, respectively. The curves are shown as functions of time.*

The improvements with fixed lag smoothing from the test presented in Fig. 14 can be seen in Fig. 22. Fig. 22b shows large improvements of the estimation

in the brake moment since the most of the peaks and dips are removed when fixed lag smoothing is applied, especially for the 2 and 5 seconds delays.

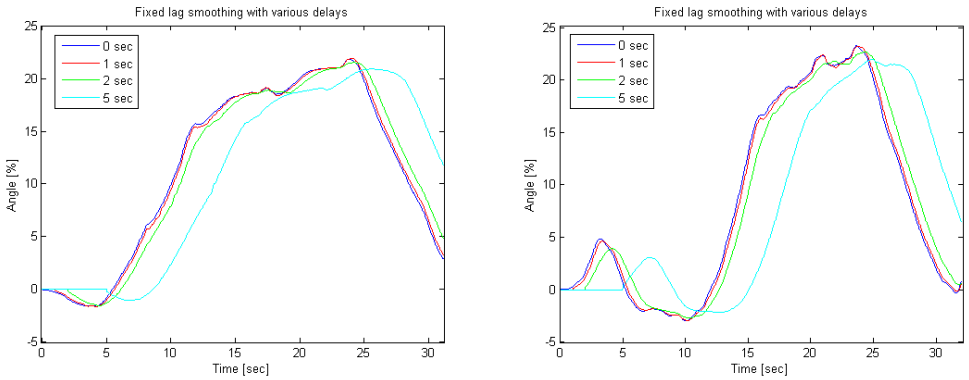

(a) *Mustang* **(b)** *Electra*

Figure 23: *Fixed lag smoothing in the 18-20 % incline, accelerating up the slope. The blue curves represent the Kalman filter estimation, i.e. without any delay. The red, green and cyan curves show the fixed lag smoothing with 1, 2 and 5 seconds delay, respectively. The curves are shown as functions of time.*

Fig. 23 shows the accelerating tests in the 18-20 % incline case with fixed lag smoothing applied. The estimations are smoother with the delays. The low-pass filter properties of the Kalman filter are obvious since the peaks and dips are removed.

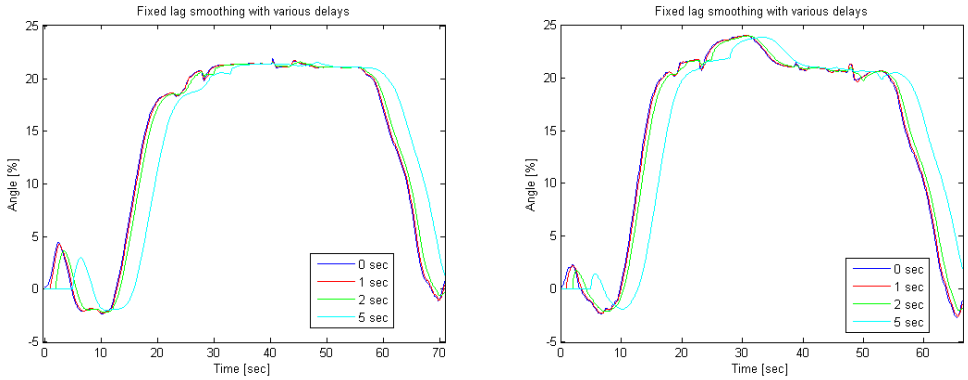

(a) *Mustang* **(b)** *Electra*

Figure 24: *Fixed lag smoothing in the 18-20 % incline, with a stop and a start in the slope. The blue curves represent the Kalman filter estimation, i.e. without any delay. The red, green and cyan curves show the fixed lag smoothing with 1, 2 and 5 seconds delay, respectively. The curves are shown as functions of time.*

As mentioned earlier, the curves from the tests presented in Fig. 19 are a bit miss-shaped since the stop took place in the 20 % part of the incline, and therefore, longer time is spent in that part. The offset behavior showed by Electra after 30 seconds in Fig. 19b is not removed with fixed lag smoothing, as seen in Fig. 24b.

4.2 Powerful retardations

Here the estimations from the brake scenarios are presented. The section starts with showing the estimations of the Kalman filter, followed by the estimations of the fixed lag smoothing with various delays. After that, a possible solution to improve the estimates is presented. The solution consists of looking at the brake pedal position and based on it, decide an appropriate covariance matrix Q, as presented in Section 3.3.4.

The brake scenarios presented in this section are from various velocities at a horizontal part of the test course, i.e. without incline. A brief comparison between Electra and Mustang is made.

In some scenarios, an external sensor, that measured the pitch of the truck, was installed. Where available, that signal is also presented.

4.2.1 Kalman filtering

In this section the estimations obtained from Kalman filtering are presented.

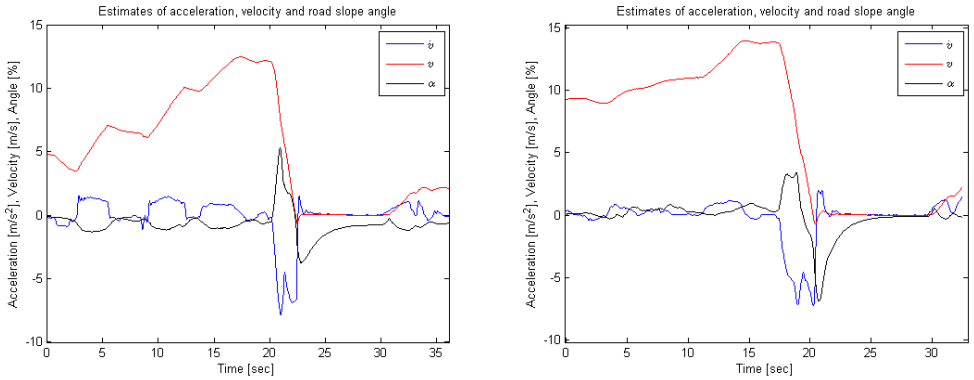

(a) *Mustang* **(b)** *Electra*

Figure 25: *Retardation on flat surface from 50 km/h. The red curves are the estimated velocities, the blue curves are the estimated accelerations and the black curves are the estimated road slope angles. The curves are shown as functions of time.*

Fig. 25 shows the estimations in a brake scenario on a flat surface without incline. Ideally the road slope angle estimation, i.e. the black curves, should be zero. That is not the case. Noticeable is that, even though Electra, in Fig. 25b, had higher velocity at the moment of retardation, the road slope angle estimation stays lower than for Mustang in Fig. 25a.

The reason that the road slope angle estimation of Mustang differs more than Electra in the acceleration part is that the acceleration with Mustang is more powerful, which can be seen by looking at both the acceleration estimate and the velocity estimate.

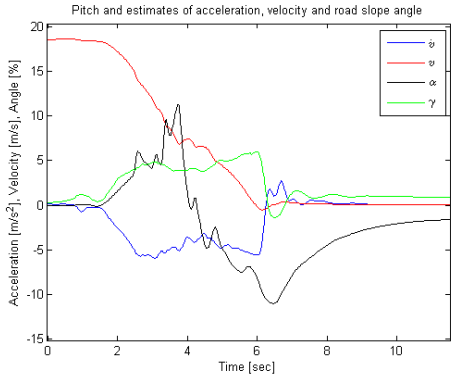

Figure 26: *Retardation on flat surface with Electra from 50 km/h. The red curve is the estimated velocity, the blue curve is the estimated acceleration and the black curve is the estimated road slope angle. The green curve represents the pitch, showed in %. The curves are shown as functions of time.*

In Fig. 26, another brake scenario from 50 km/h with Electra is shown. Here is also the pitch presented. It can be seen that the pitch, represented by the green curve, has a strong coupling with the acceleration of the truck, shown in the blue curve. The road slope estimation is more than 10 % during the retardation, even though the road was horizontal.

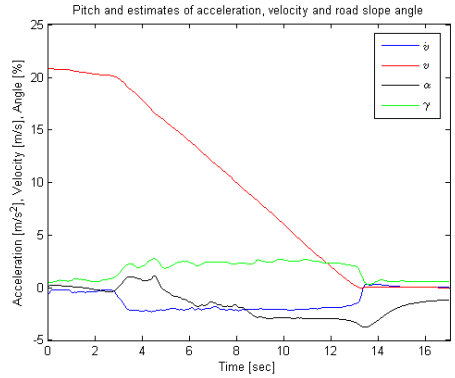

Figure 27: *Retardation on flat surface with Electra from 60 km/h. The red curve is the estimated velocity, the blue curve is the estimated acceleration and the black curve is the estimated road slope angle. The green curve represents the pitch, showed in %. The curves are shown as functions of time.*

Fig. 27 shows a brake scenario from 60 km/h. The retardation here is not as powerful as the other scenarios presented in this section. This can be seen

by looking at the acceleration, which is only -2 m/s^2 here, instead of -5 m/s^2 as in the other retardations. This does not cause the truck to pitch as much, which is beneficial to the road slope estimation. The road slope estimation varies from 2 % to -3 %.

Another idea as to why the road slope estimation is much better in this case, is that the elements in the covariance matrix Q are quite low, which makes the system more appropriate for less powerful retardations, than more powerful ones. The elements are chosen in order to obtain good results in all driving scenarios, not just the retardations.

As explained in Section 3.3.2, the covariance matrix Q is adjusted for an acceleration/retardation of about 3 m/s^2.

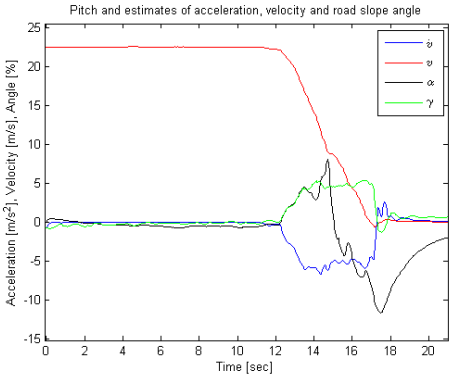

Figure 28: *Retardation on flat surface with Electra from 75 km/h. The red curve is the estimated velocity, the blue curve is the estimated acceleration and the black curve is the estimated road slope angle. The green curve represents the pitch, showed in %. The curves are shown as functions of time.*

A fairly powerful retardation with Electra from 75 km/h is presented in Fig. 28. The retardation hits a maximum of -6 m/s^2. This causes the truck to pitch more than in the previously presented retardation. The estimation of the road slope varies from 8 % to -12 %.

4.2.2 Fixed lag smoothing

In this section, the improvements obtained with fixed lag smoothing are shown for the same brake scenarios as presented in the previous section. To get a better overview of the curves, only road slope estimations are presented, and not the other states.

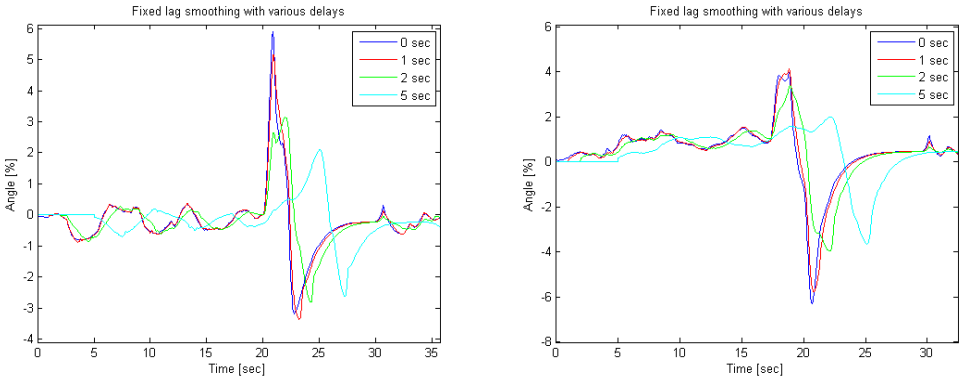

(a) *Mustang* **(b)** *Electra*

Figure 29: *Retardation of -6 m/s^2 on flat surface from 50 km/h when fixed lag smoothing is used. The blue curves represent the Kalman filter estimation, i.e. without any delay. The red, green and cyan curves show the fixed lag smoothing with 1, 2 and 5 seconds delay, respectively. The curves are shown as functions of time.*

The improvements for the brake scenario presented in Fig. 25 can be seen in Fig. 29.

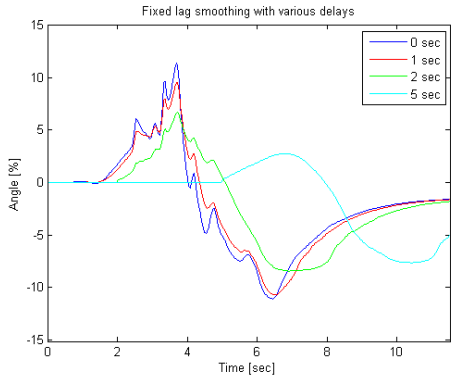

Figure 30: *Brake scenario of -5 m/s^2 with Electra from 50 km/h with fixed lag smoothing. The blue curve represents the Kalman filter estimation, i.e. without any delay. The red, green and cyan curves show the fixed lag smoothing with 1, 2 and 5 seconds delay, respectively. The curves are shown as functions of time.*

Fig. 30 shows a retardation from 50 km/h with Electra when fixed lag smoothing is used. The estimation are seen to improve as the the delay increases.

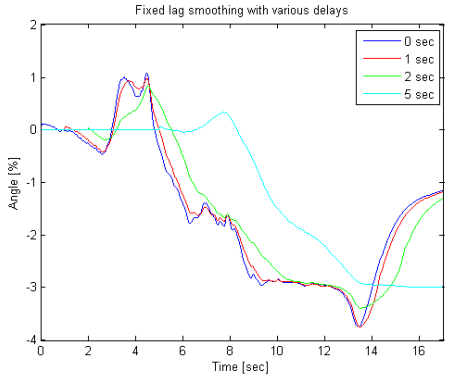

Figure 31: *Brake scenario of -2 m/s^2 with Electra from 60 km/h with fixed lag smoothing. The blue curve represents the Kalman filter estimation, i.e. without any delay. The red, green and cyan curves show the fixed lag smoothing with 1, 2 and 5 seconds delay, respectively. The curves are shown as functions of time.*

In Fig. 31, the less powerful brake scenario from 60 km/h is shown. Note that the scale on the axis that shows the incline is different.

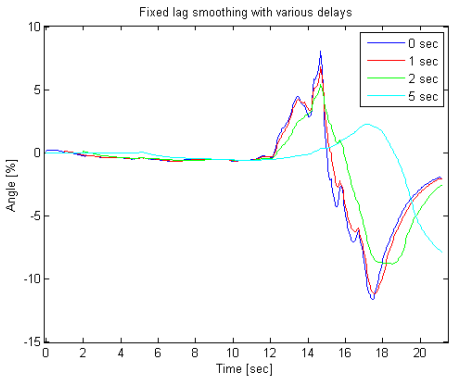

Figure 32: *Brake scenario of -5 m/s^2 with Electra from 75 km/h with fixed lag smoothing. The blue curve represents the Kalman filter estimation, i.e. without any delay. The red, green and cyan curves show the fixed lag smoothing with 1, 2 and 5 seconds delay, respectively. The curves are shown as functions of time.*

Fig. 32 presents the road slope estimation from the rather powerful retardation from 75 km/h with Electra. It can be seen that with 2 seconds delay, shown in the green curve, the improvements are as much as 5 percentage points.

4.2.3 Covariance matrix change

In this section, the covariance matrix Q is changed by looking at the brake pedal position, according to the solution presented in Section 3.3.4.

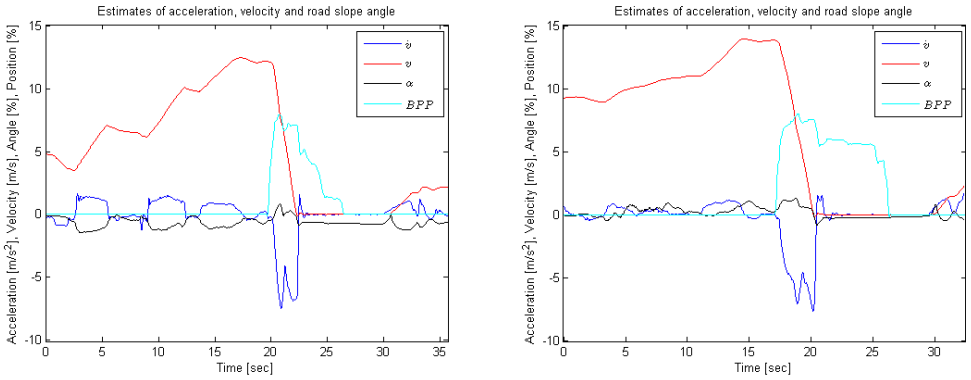

(a) *Mustang* **(b)** *Electra*

Figure 33: *Retardation of -6 m/s^2 on flat surface from 50 km/h when the covariance matrix Q is changed with regards to the brake pedal position. The blue curves show the estimated acceleration, the red curves show the estimated velocity and the black curves represent the estimated incline. The cyan curves show the brake pedal position in 0.1·%. The curves are shown as functions of time.*

Fig. 33 shows the estimations of the system where the covariance matrix Q is changed when a retardation is detected. The retardation is detected by looking at the brake pedal position. When the brake pedal is at 25 % of its maximum position, the covariance matrix is changed so that the estimation of road slope is not as sensitive to changes.

Comparison with Fig. 25 shows that the estimation of the velocities and accelerations stays the same, regardless of the change in the elements in the covariance matrix. It can also be seen that the incline estimations stay much closer to zero, which is the aim here.

4.3 Horizontal turns

This section presents a few driving scenarios on flat ground to investigate the influence of horizontal centripetal acceleration.

No fixed lag smoothing is presented here. The reason is that the data might be corrupt, which is elaborated in Section 6.5, and any improvements gained with fixed lag smoothing are irrelevant.

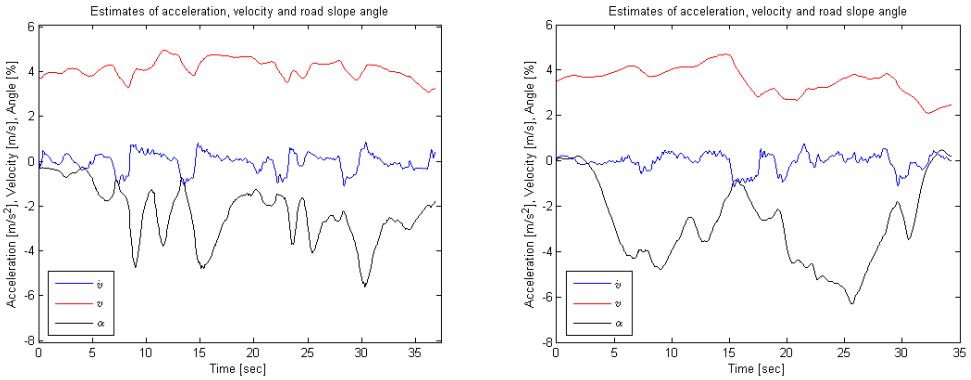

(a) *Electra, left turns* **(b)** *Electra, right turns*

Figure 34: *Two full horizontal turns shown as functions of time. The red curves show the estimated velocities, the blue ones the estimated accelerations and the black curves represent the estimated road slope angles.*

Fig. 34 shows the results obtained from a test where the influence of centripetal acceleration in horizontal turns was investigated. The test drives were done in circles on flat ground. Maximum steering wheel angle was used at both tests.

It can be seen that the road slope estimations are negative regardless of direction of the turn. Ideally, the road slope estimations should be zero.

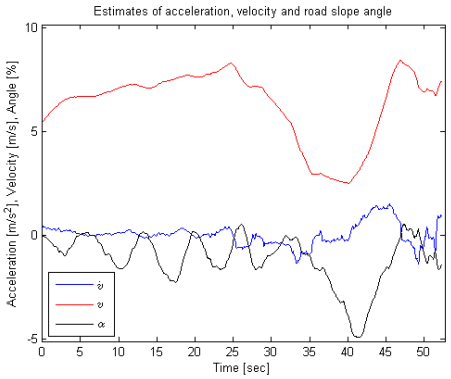

Figure 35: *A test drive where the motion of a snake was driven, and ended with a full 180 degree turn. The red curve shows the estimated velocity, the blue one the estimated acceleration and the black curve represents the estimated road slope angle.*

Fig. 35 shows a driving scenario on flat ground where a lot of turns were made. The drive was meant to simulate the motion of a snake, in order to investigate the influence of horizontal centripetal acceleration. The test ended with a full 180 degree turn. That part can easily be identified in the figure since the velocity was lowered.

The test gave an inaccurate incline estimate, since the road used for the test was horizontal.

Either the assumption that the horizontal centripetal acceleration does not affect the longitudinal accelerometer is wrong, or the acceleration measured is due to the icy road during testing.

4.4 Real driving simulation

In this section, no fixed lag smoothing was needed to obtain a good estimation, and therefore it is not presented.

Note that these tests are longer and the scale on the time-axis is different from the previously shown tests.

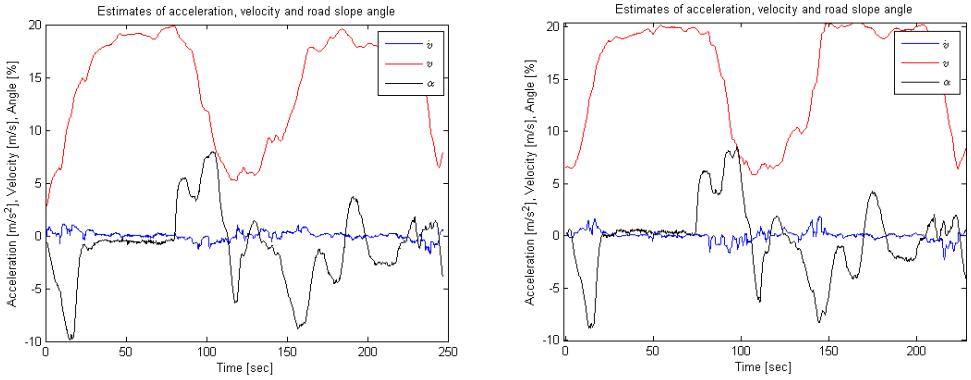

(a) *Mustang* **(b)** *Electra*

Figure 36: *The first part of the test course. The red curves are the estimated velocities, the blue curves are the estimated accelerations and the black curves are the estimated road slope angles. The curves are plotted as functions of time.*

In Fig. 36, the results from the first part of the test course are presented. This drive scenario was meant to simulate real driving. The drive included both uphill and downhill slopes, which can be seen by looking at the road slope estimation. The estimations follow the available data on the test course very well.

The estimations of both Electra and Mustang show here a very similar behavior. The influence of Electra's air suspension does not show as much in these tests. Even though the sensors were calibrated before the estimations are made, Mustang shows an offset appearance in Fig. 36a.

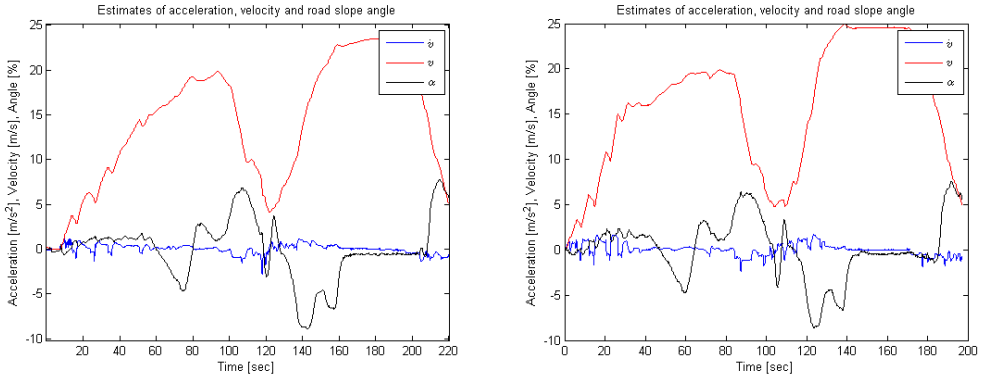

(a) *Mustang* **(b)** *Electra*

Figure 37: *The second part of the test course. The red curves are the estimated velocities, the blue curves are the estimated accelerations and the black curves are the estimated road slope angles. The curves are plotted as functions of time.*

Fig. 37 shows the estimations on another part of the test course, also with both uphill and downhill slopes. The road slope estimations of the two trucks show very similar behavior here, as well.

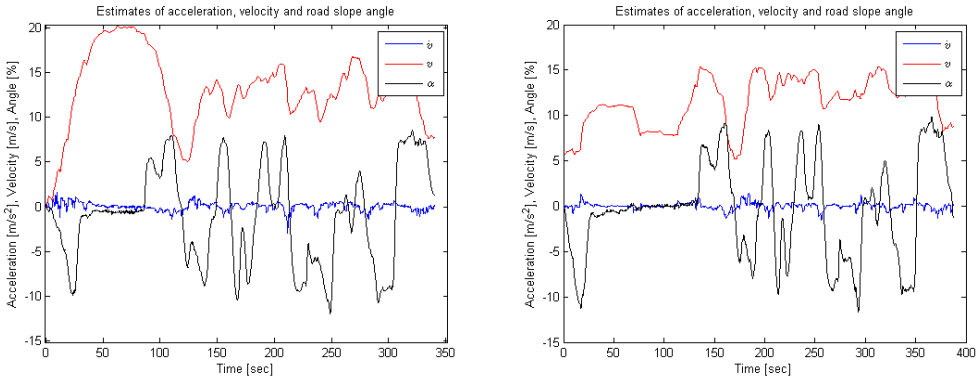

(a) *Mustang* **(b)** *Electra*

Figure 38: *The third part of the test course. The red curves are the estimated velocities, the blue curves are the estimated accelerations and the black curves are the estimated road slope angles. The curves are plotted as functions of time.*

As can be seen in Fig. 38, the estimation of road slope shows a similar behavior with the two trucks. It can be seen that in the drive with Electra in Fig. 38b the velocity, represented by the red curve, had to be altered from the drive done with Mustang in Fig. 38a. This was due to other traffic on the test course.

4.5 Comparison with GPS-data

This section presents GPS-data for chosen parts of the test course. This data is used for comparison with the estimations obtained. According to [14], the accuracy of the GPS-receiver used for this validation is 10 centimeters and the distance is calculated from coordinates with CSG Network's converter [8].

The data used for comparison in the inclines are from the test drives with Electra at 25 km/h.

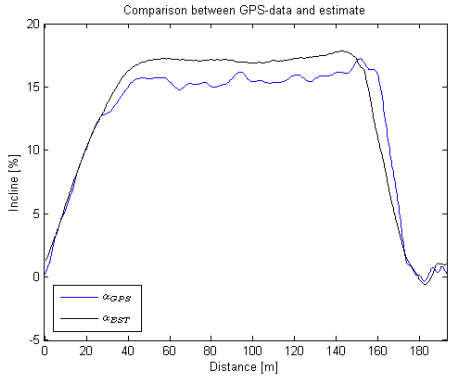

Figure 39: *Comparison in the 16 % slope. The GPS-data is shown in blue and the estimation in black, as functions of distance.*

Fig. 39 shows both the estimation of Electra in the 16 % slope as well as the incline calculated from the GPS-data. The ratio between the curves is about 0.83, and can be calculated by dividing the GPS-data with the estimation,

$$\frac{15}{18} = 0.8333, \tag{4.1}$$

which means that the road slope angle is 83 % of the obtained estimation.

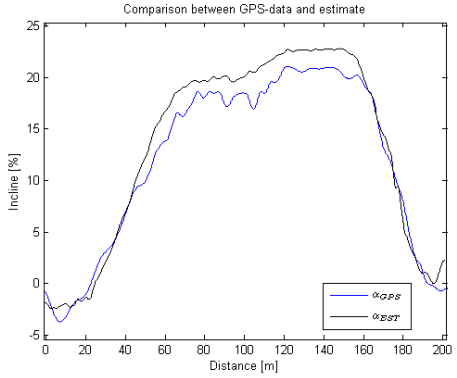

Figure 40: *Comparison in the 18-20 % slope. The GPS-data is shown in blue and the estimation in black, as functions of distance.*

In Fig. 40, a comparison between the estimation obtained with Electra at 25 km/h and the GPS-data in the 18-20 % incline is shown. In the same way as above, the proportional error can be calculated as a ratio between the

incline from the GPS-data and the estimation for both parts of the incline. The ratio in this case is 0.9 and 0.87, which corresponds to 90 % and 87 %, respectively. The calculations made are

$$\frac{18}{20} = 0.9, \quad \frac{20}{23} = 0.8696. \tag{4.2}$$

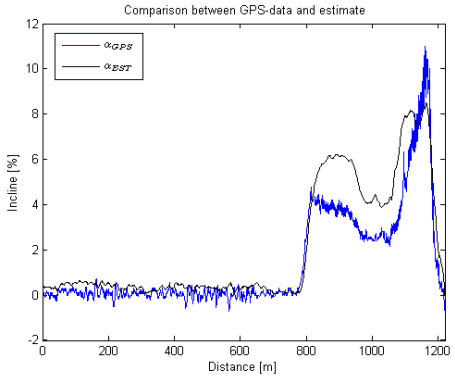

Figure 41: *Comparison in a part on the test course where the road is horizontal, then increases to 6 %, decreases to 4 % and ends with an incline of 8 % before it becomes horizontal again. The GPS-data is shown in blue and the estimation in black, as functions of distance.*

Fig. 41 shows the road slope estimation of Electra and the incline calculated from GPS-data. The proportional errors in this case differs a lot, which is seen in Eq. 4.3.

$$\frac{4}{6} = 0.6667, \quad \frac{2.5}{4} = 0.625, \quad \frac{10}{8} = 1.25 \tag{4.3}$$

This mean that the road slope angle is 67 %, 62 % and 125 % of the obtained estimation, respectively. If the assumption made in Section 3.2.1 were correct, the ratio would be 1, i.e. 100 %.

5 Discussion and Conclusions

The model proved to generate an accurate estimate of the road slope angle. The model gives a fast response and is appropriate for a real-time application.

The filter is adjusted as a compromise to generate an accurate estimation in all scenarios. The estimations can be improved slightly by adjusting the covariance matrices with regards to specific driving scenarios. If fast and accurate estimations in the inclines are wanted, the elements of the covariance matrix Q can be increased. This allows the signal to drift more between the samples. Unfortunately, this mean that the retardation scenarios will suffer even worse estimations. But if these scenarios can be solved in another way, a few suggestions can be found in Section 7, this might be a solution.

5.1 Inclines

As seen in Section 4.1, the estimations of road slope angle in the inclines are rather accurate. The inaccuracy presented is mainly when the velocity is changed. Constant velocity gives an accurate estimation. The problem in velocity changes is probably caused by the pitch of the truck or due to the phase difference between the signals, which is presented in Section 6.3.

The estimations have a proportional error of a few percent. The estimations of Electra is consistently higher than Mustang, this is probably due to the fact that Electra has air suspension and is more prone to pitch. This is also covered briefly in Section 2.3.

The estimations during the accelerating tests up the inclines proved to be quite robust when compared to the other estimations obtained in the respective incline. The comparisons are seen in Fig. 15 and Fig. 20. Only the test with a stop in the 16 % incline with Electra stands out. The estimation shows an offset after the stop, which also happens in the same test in the 18-20 % incline, which can be seen in Fig. 20. The reason for this behavior has not been explained, but could be because of the air suspension system.

Fixed lag smoothing were showed to improve and smoothen the estimations where it was needed. The 2 second delay were shown to remove the worst peaks in the estimations. 1-2 seconds seems to be a reasonable delay compared with the increased accuracy gained.

5.2 Powerful retardations

Section 4.2 showed that the road slope estimations are inaccurate in retardation scenarios. The fixed lag smoothing increased the accuracy, but not enough. Therefore, a solution, where the covariance matrix Q was changed,

was tested in an attempt to improve the estimations further.

The inaccuracies could be due to a phase shift between the signals of which the estimation is based on. This subject is elaborated in Section 6.3.

In some scenarios, the pitch was also presented. As it can be seen in that the pitch is strongly coupled with the vehicle acceleration $\dot{v}$, but not the road slope estimation.

A solution for improvement of the estimation in brake scenarios were presented. The solution consisted of changing the covariance matrix Q when the brake pedal is more than 25 % of its maximum position. By doing so, the estimation kept its current value and not allowed to change as much between the samples. The two first elements of the matrix, i.e. $\dot{v}$ and v, are increased ten times, and the last state, g_x, is decreased ten times. These values are obtained by tuning, and have no further motivation. Fig. 33 shows that the improvement was successful. The road slope estimations stay closer to zero than with the original covariance matrix.

With this solution, the convergence back to the real value might take some time since the incline estimation is slowed down. A question that comes to mind is if the incline estimation has to be correct in a brake scenario. Is it not better to have an inaccurate estimate during the retardation, but an accurate one when it is time to start again, so that an appropriate starting gear can be chosen?

In Fig. 33a, Mustang shows an offset of about 1 % in the incline estimation. The behavior can also be seen in Fig. 25a, but can not be explained.

5.3 Horizontal turns

In theory, the estimations presented in Section 4.3 should be zero. The lateral and centripetal acceleration caused by these tests should not affect the longitudinal acceleration. The inaccurate estimations are probably caused by the icy road, which is further elaborated in Section 6.5. When the truck skidded, a longitudinal acceleration was created. This acceleration was measured by the accelerometer and gave rise to an incorrect road slope estimation.

No explanation can be thought of as to why the estimations are negative regardless of direction of the circles.

5.4 Real driving simulation

The test course had to serve as real driving simulation. The estimation of road slope angle are shown to handle this simulation very good. It follows

the information available regarding the slopes on the course well.

One conclusion that can be made from the results in Section 4.4 is that the type of suspension does not matter. Both Mustang and Electra, with steel suspension and air suspension, respectively, show equally good estimations. In steep inclines and during powerful retardations, there is a larger difference between the two trucks.

Disturbing is that, even though the data was calibrated to remove offsets, there is an offset error on Mustang in some of the horizontal parts of the course.

5.5 Comparison with GPS-data

Section 4.5 showed GPS-data for chosen parts of the test course. The linear ratios from the comparisons were presented. The data presented contained high resolution altitude information.

Disturbing is that the linear ratio assumed to be between the truck angle and the road slope angle differs between the different scenarios presented in Section 4.5.

At first, the ratio is calculated to be about 0.85. This corresponds to that the road slope angle is 85 % of the truck angle. But Fig. 41 shows otherwise. In the first two inclines, the ratio is calculated to be about 0.65, but in the last incline the ratio is 1.25, which corresponds to 65 % and 125 %, respectively.

If this GPS-data is to be used for validation, the assumption that the road slope angle equals the truck angle, i.e. the pitch equals zero, is wrong. Still it is very hard to decide a ratio as it differs between the scenarios, and one can not be sure of that it is correct without proper validation.

The estimations follows the data available on the inclines of the test course very well. The data suggests that the incline is 6 %, then 4 % and ends with an angle of 8 %. But the GPS-data presented in Section 4.5 gives different inclines. According to the GPS-data, the inclines are 4 %, 2.5 % and 10 %.

Noticeable is that the GPS-data gives the same road slope angle as the available data in the slopes tested, 16 % and 18-20 %.

6 Problems

In this chapter, some problems that occurred along the way will be discussed. Also, a few ideas of possible solutions are presented.

6.1 Validation

The main problem throughout the thesis has been the lack of validation. This is due to inadequate information on existing road slope angles.

One approach to solve this was by looking at GPS-data. Unfortunately, the receivers used during the sampling of data lacked the requested altitude accuracy for a reliable validation. However, GPS-data with high altitude accuracy was available. By investigating it, validation was possible to a certain extent.

Another idea to validate the estimation, was to use a traditional elevation meter, which calculates the elevation from the change in atmospheric pressure. This approach was discarded due to inadequate accuracy at these sensors.

6.2 Obsolete vertical sensor

Before the collecting of data, an additional sensor was attached to the trucks. The sensor was an accelerometer which measured the acceleration in the vertical direction. This additional sensor was installed for the purpose of validating the estimated slope.

Unfortunately, what was not taken into consideration was that the vertical sensor determines g_z as a function of $\cos(\alpha)$:

$$g_z = g \cdot cos(\alpha). \tag{6.1}$$

This lead to that the data from the vertical sensor was unusable due to the nonlinear characteristics of the *cosine* function. The *sine* function, which was used throughout the thesis, is also nonlinear, but in a beneficial way. This is described graphically in Fig. 42.

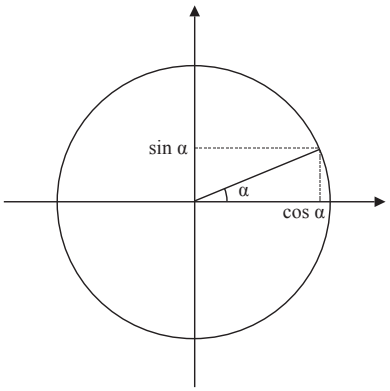

Figure 42: *Comparison between the sine and cosine functions for a given angle* α*.*

As can be seen in Fig. 42 the angle α is the same but generates a much bigger difference in how it is amplified through the *sine* and *cosine* functions. The *sine* function is covering a much larger interval, and therefore has the ability to be more accurate. The *cosine* function is still close to 1, even though the angle α is quite large. A conclusion of this is that the angle originating from the *sine* value is easier to determine. The value from *cosine* is not large enough, considering the added noise, to be used for validation.

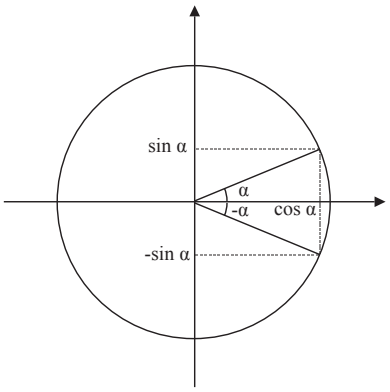

Figure 43: *Comparison between the negative values for the sine and cosine functions for a given angle* α*.*

Another problem that would occur with this sensor is that it can not tell the difference between an uphill slope and a downhill slope. This is also due

to the properties of the *cosine* function. Since $\cos(\alpha) = \cos(-\alpha)$, the value of the function would be the same, independent of the sign of the angle α. Compared to the *sine* function, where $\sin(\alpha) = -\sin(-\alpha)$, i.e. the sign of the angle follows with the function. This can be seen in Fig. 43.

6.3 Phase difference

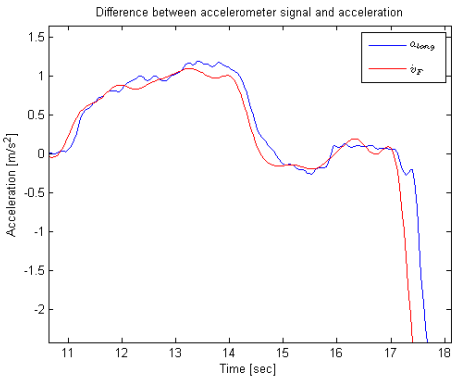

Figure 44: *Phase difference from the braking done with Electra from 50 km/h. The blue curve shows the signal from the accelerometer, and the red one a filtered version of $\dot{v}$. The curves are shown as functions of time.*

One idea why the estimations in the brake scenarios are so inaccurate is that there is a phase difference between the signal from the accelerometer and the acceleration of the vehicle. The difference between the signals, from which the road slope estimation is made, starts out positive.

Attempts of solving this problem were performed unsuccessfully. As can be seen in Fig. 44, the delay is about 0.20 seconds.

6.4 ABS-influence corrupted data

One of the many different driving scenarios tested in this thesis is how the accelerometer, and therefore the road slope estimation, is effected by a powerful retardation.

As seen in Section 3.2, the acceleration $\dot{v}$ is an important part of the model. The acceleration signal is based upon the individual front wheel velocities, which are combined to get an average velocity of the vehicle and then derived to obtain the vehicle acceleration. During the retardation, one of the front wheels was locked due to the influence of the Anti-lock Brake System (ABS).

The ABS makes sure that the vehicle comes to a stop as quick as possible by maximizing the friction between the road and the tires by applying the appropriate brake pressure and distributing the brake power optimally between the wheels to make sure no wheel is skidding. If a wheel locks during the braking, the velocity signal, and therefore the acceleration signal, is corrupted and is not good enough to base an estimation on.

Therefore, in some cases, the signal had to be adjusted manually, by adding data, to make sure that the signal was of the requested quality.

6.5 Icy roads during horizontal tests

In the ideal case, a vehicle with constant velocity is only affected by a horizontal centripetal acceleration in a turn. When the tests in Section 4.3 were carried out, the road was very slippery due to ice. The slip gave rise to a longitudinal acceleration that normally is not there.

Because of this, the estimations obtained in that section is probably worse than if the grip had been better. To include the slip angle in the model is not necessary since this rarely happens.

7 Future Work

As can be seen from the results presented in Section 4, the correct road slope angle can be obtained if the conditions are right. Different driving scenarios give different results. In order to make the system more robust and capable of handling all driving scenarios, a few developments are needed. These are presented in this chapter.

7.1 Extending the model

One way to improve the estimations would be to extend the model and include the pitch signal. Since this signal is not available for measurement today, this thesis did not include it in more than in a few measurements.

7.1.1 Including the pitch

A sensor that measured the pitch of the truck could greatly improve the results, especially in the retardations. The complete equation of the system could be [12]:

$$a_{long} = \dot{v}_x + g_x + \dot{\gamma}z + \ddot{\gamma}v_x, \tag{7.1}$$

where γ is the pitch angle, $\dot{\gamma}$ is the pitch-rate, $\ddot{\gamma}$ is the pitch-acceleration, z is the distance the truck pitches and v_x is the velocity of the truck.

There are advanced methods to model the pitch, but since the goal is to create a real-time application, computations must be kept to a minimum. Therefore, this solution was discarded.

One way of minimizing the computational power required, is to assume that there is a linear relationship between the angle of the truck and the road slope angle. The ratio could be calculated by looking at the estimated truck angle compared to a known incline. This is not a reliable way of solving the problem since the ratio will depend on the properties of the truck, such as axis distance and type of suspension, as well as changeable parameters, such as weight and center of gravity. Another problem with this solution is that it is very hard to know the exact incline since there is a lack of information in this area.

7.1.2 Linear ratio

The improvement of the estimation that can be achieved with a linear approximation of the road slope angle from the truck angle has to be further

investigated. What must be investigated is the affects of the ratio from e.g. the weight and center of gravity of the vehicle.

7.2 When should the filter be active?

As mentioned in Section 5.2, the values found for the covariance matrix Q are tuned. More testing has to be done in order to find the optimal values for this kind of solution.

Perhaps two intervals of the brake pedal position for the change is needed, e.g. at 25 % and 50 %. By doing so, the more powerful retardations are seperated from the less ones. The elements in the covariance matrix Q have to be changed accordingly.

Another problem is when a truck equipped with air suspension changes the horizontal level. This will influence the results of the road slope estimation and precautions must be taken.

7.3 Phase difference

The phase difference between the accelerometer signal and the acceleration, explained in Section 6.3, and its influence on the estimation, has to be further investigated. By making sure these signals are in phase, it might be possible that the solution stated above is not needed, nor the extension of the model.

7.4 ABS-influence

As described in Section 6.4, the velocity signals had to be adjusted manually due to influence of ABS. If the real-time application is to be based on the same velocity signals mentioned here, the same problem could occur. The velocity used in this thesis is used upon the individual wheel velocities.

One way to get around this is to use velocity derived from the GPS-position. Another way would be to detect when the ABS is active, and make the appropriate changes to the system.

7.5 Estimate the zero-level

To obtain an accurate estimation, the zero-level, i.e. where the ground is horizontal, must be known. Throughout this thesis, correct zero-level has been assumed. This was achieved by calibrating the accelerometer before the estimation is done, which is mentioned briefly in Section 3.2.1.

For a real-time application, a recursive estimation should be made, since it is not possible to calibrate the data in this way every time the load is changed or the properties of the truck is changed in another way.

7.6 Trailers

The effects of a trailer in combination with a tractor must be investigated since this was not tested in this thesis.

Intuitively, the effect of the trailer should not matter. The trailer increases the weight of the carriage, but the weight is not included in this model since it is not assumed to affect the road slope estimation.

Furthermore, since the trailer causes the tractor to pitch less it is probably beneficial to a road slope angle estimation. What might influence the accuracy of the estimation is if the tractor is weighted down by the trailer so the truck angle is not horizontal. But this will probably not influence the results either since a tractor with air suspension makes sure that the vehicle stays horizontal by controlling pumps and valves. A tractor with steel suspension is stiff enough to manage the increased weight [15].

7.7 Construction vehicles

One must investigate what happens to construction vehicles that uses road without the standards mentioned in Section 2.4.

The challenges include decreased radius of the vertical curves and steeper inclines. The road slope estimation for this kind of vehicle could be used to choose an appropriate starting gear.

7.8 Real-time application

A real-time application has to be developed in order to make the estimations in real-time in the trucks. The model presented in this thesis can be implemented in Simulink.

References

[1] F. Gustafsson, L. Ljung and M. Millnert: *Signalbehandling*, 2nd Edition, Studentlitteratur 2000, 2001

[2] G. Welch and G. Bishop: *An introduction to the Kalman Filter*, Department of Computer Science, University of North Carolina at Chapel Hill, 2006

[3] R. E. Kalman: *A New Approach to Linear Filtering and Prediction Problems*, Transaction of the ASME – Journal of Basic Engineering, pp. 35-45, March 1960

[4] D. Simon: *Kalman Filtering*, Embedded Systems Programming, pp. 72-79, June 2001

[5] Näringsdepartementet: *Förordning (2008:1380) med instruktion för Vägverket*, 3 §, December 2008

[6] Vägverket: *Vägar och gators utformning, Linjeföring*, Vägverket Publikation 2004:80, pp. 101-106, May 2004

[7] Vägverket: *Vägar och gators utformning, Grundvärden*, Vägverket Publikation 2004:80, May 2004

[8] GPS Converter: *http://www.csgnetwork.com/gpsdistcalc.html*, CSG Network, Version 6.2.1

[9] P. Berglund, B. Hanner, M. Backholm and P. Salberg *Coordinates Systems - Trucks* Scania CV AB, Standard STD4083, Issue 3, 15 December 2008

[10] M. Blundell and D. Harty *The Multibody Systems Approach to Vehicle Dynamics* Butterworth-Heinemann LTD, 2004

[11] Sten Lundgren *RTC, Scania CV AB*. Private communication.

[12] Jolle Ijkema *RTCD, Scania CV AB*. Private communication.

[13] Pär Degerman *REP, Scania CV AB*. Private communication.

[14] Rickard Lyberger *REP, Scania CV AB*. Private communication.

[15] Ines Kasumovic *REVC, Scania CV AB*. Private communication.